Journal of Materials Chemistry A

REVIEW

View Article Online
View Journal | View Issue

Check for updates

Cite this: J. Mater. Chem. A, 2024, 12, 16268

Anode-free lithium metal batteries: a promising flexible energy storage system

Kai Tang,† Liying Tian,† Yuwei Zhang and Zhichuan J. Xu *

The demand for flexible lithium-ion batteries (FLIBs) has witnessed a sharp increase in the application of wearable electronics, flexible electronic products, and implantable medical devices. However, many challenges still remain towards FLIBs, including complex cell manufacture, low-energy density and low-power density. To address these issues, researchers have widely conducted studies on the structure and material design of flexible batteries. Among these efforts, the anode-free lithium metal battery (AFLMB) stands out as a promising solution, offering potential new avenues for research in flexible battery design. The anode-free full cell configuration removes excess lithium and combines the fully lithiated cathode with a bare current collector (CC), which not only simplifies the production process and lowers the cost, but also achieves light weight and high-energy-density. Nevertheless, AFLMBs are still confronted by challenges including diminished coulombic efficiency (CE), shortened cycle longevity, and lithium dendrite growth, which substantially impede the practical application of AFLMBs towards flexible batteries. This review provides an overview of the latest developments in anode-free batteries, particularly focusing on research strategies in electrolyte design and current collector modification. Considering the characteristics of flexible batteries, the article also points out the challenges and feasible research directions for the development of flexible AFLMBs. It is concluded that although there are significant challenges in developing flexible AFLMBs, the design of gel electrolytes and polymer artificial solid electrolyte interphases (SEIs) can expedite practical advancements, aiming to achieve safe, light weight, cost-effective, and high-energy-density flexible batteries.

Received 26th March 2024
Accepted 30th May 2024

DOI: 10.1039/d4ta02003k

rsc.li/materials-a

Open Access Article. Published on 14 juin 2024. Downloaded on 2025-01-24 19:52:32.
This article is licensed under a Creative Commons Attribution-NonCommercial 3.0 Unported Licence.

1. Introduction

The relentless pursuit of sustainable and efficient energy sources in recent decades has catalyzed significant scientific inquiry and technological development in the field of green energy. Among the various technological breakthroughs, lithium-ion batteries (LIBs) with high power and energy density, a nearly zero-memory effect and long cycle life, have emerged as the major electrical energy storage system. They showcase their immense application potential and value across a wide spectrum, ranging from large-scale grid energy storage and electric vehicles to small-sized medical devices and portable electronic products. Among numerous LIB types, flexible LIBs (FLIBs) have been widely developed as demand increases for novel flexible electronic products such as wearable and implantable medical devices. Compared to traditional LIBs, FLIBs have significant advantages in resisting mechanical deformation. They can withstand bending, stretching, twisting, and folding without compromising their original battery performance. Therefore, FLIBs enable electronic products to exhibit excellent performance under severe conditions. However, flexibility is just one of the key parameters of FLIBs. To make FLIBs more competitive, the manufacturing of FLIBs must utilize low-cost materials and manufacturing methods. Additionally, FLIBs should also possess characteristics such as high energy density and power density, light weight, and high safety.

To enhance the performance of flexible batteries, designing novel battery structures has become a crucial research direction. Currently, various flexible cell configurations, such as coplanar, cable and node-type, have been developed. These unique structures can accommodate high deformation states while ensure outstanding electrochemical performance. However, many of these novel battery structures are primarily designed to enhance their mechanical performance, often neglecting metrics such as lightweighting and energy density. The concept of anode-free lithium metal batteries (AFLMBs) introduces a fresh perspective to battery structure design, eliminating the need for an initial lithium anode.[1,2] This approach achieves both light weight and increased energy density while also reducing battery production costs, making it an ideal system for flexible batteries.

The cycling stages of AFLMBs are depicted in Fig. 1, which offer a promising alternative to conventional lithium-ion batteries by eliminating the use of the traditional lithium

School of Materials Science and Engineering, Nanyang Technological University, Singapore. E-mail: xuzc@ntu.edu.sg

† These authors contributed equally.

This journal is © The Royal Society of Chemistry 2024

Open Access Article. Published on 14 juin 2024. Downloaded on 2025-01-24 19:52:32.
This article is licensed under a Creative Commons Attribution-NonCommercial 3.0 Unported Licence.

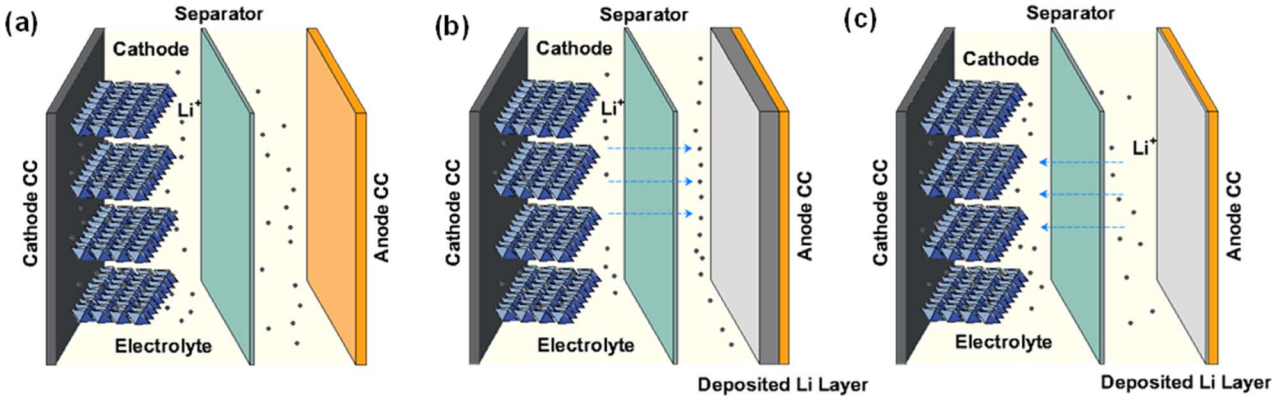

Fig. 1 The basic mechanism of anode-free lithium metal batteries. (a) Schematic of AFLMBs. (b) Charge and (c) discharge processes of AFLMBs.

anode. During the cell charge process, lithium ions are stripped from the cathode, migrate across the electrolyte, and deposit onto the anode current collector, creating a lithium layer. In the subsequent discharge process, the lithium ions shuttle back to the cathode, maintaining the energy cycle of the AFLMB. Despite AFLMB's structural advantages mentioned above, its practical application is hindered by poor reversibility of lithium deposition and stripping. Additionally, "mossy" lithium dendrites with high surface area grow severely and are prone to detachment from the substrate, leading to the formation of dead lithium during discharge processes and further causing rapid capacity degradation.

The severe growth of lithium dendrites and poor coulombic efficiency are also critical issues limiting the application and development of AFLMBs in flexible devices.[3,4] Inactive materials used in battery manufacturing, including electrolytes and current collectors, play crucial roles in stabilizing lithium deposition and maintaining lithium inventory. Simultaneously, current collectors are employed to provide structural support for flexible battery electrodes and establish conductive pathways for active battery materials, thereby playing significant roles in ensuring both flexibility and stability.[5–8] Consequently, the development of flexible AFLMBs should focus on the current status of electrolytes and current collectors, their interactions, and the latest advancements that may benefit the field of flexible batteries.

The review focuses on the latest breakthroughs in electrolytes and current collectors, aiming to promote the application of flexible AFLMBs. The discussion will traverse the critical parameters of coulombic efficiency and capacity retention, which are indicative of AFLMB systems' cycling stability and the reversibility of lithium. In addition, a special focus is given to novel electrolyte categories with their intrinsic features. And the lithium nucleation overpotential is emphasized, which is considered a crucial determinant of the compatibility between the current collector and lithium. The review concludes by emphasizing performance and manufacturing process-related challenges relevant to the practical application of flexible lithium-based batteries, providing strategies for achieving practical applications of flexible lithium-based batteries, thus presenting a realistic outlook.

2. Electrolyte design to extend cycling life of AFLMBs

2.1 The role and evolution of electrolytes

The kinetics of Li nucleation and growth are heavily impacted by the composition of electrolyte, indicating the significance of developing electrolyte for achieving AFLMBs with exceptional performance.[9] Electrolytes in battery systems serve a dual role: they are the conduit for ionic conduction, allowing for the transfer of lithium ions between the cathode and anode during charge and discharge cycles, and they are instrumental in the formation of the solid-electrolyte interphase (SEI). The SEI is a nanostructured layer formed on the surface of the electrode, and its composition, morphology and stability are critical for the overall performance of the battery. This interphase acts as a selective membrane that allows the passage of lithium ions while blocking electrons, which is vital for preventing short-circuiting and thermal hazards. Furthermore, an uneven SEI will result in a non-uniform diffusion rate of lithium ions, leading to uneven Li deposition. Progress has been made from the early stages of battery development using simple electrolytes to the current development of very complex electrolytes.[10] Initial electrolytes are generally reactive and unstable, leading to erratic SEI formation and poor cycling life. Over time, as the understanding of SEI dynamics increased, the focus shifted to designing electrolytes capable of forming a stable SEI with high lithium-ion conductivity and low reactivity to lithium metal.[11]

In AFLMBs, the role of the electrolyte and SEI will be more evident where there is no lithium intercalation host to buffer the lithium plating process. An ideal electrolyte for AFLMBs should prevent lithium metal dissolution, promote lithium-ion flow, and create an SEI that can dynamically adjust itself when the volume of the cell is fluctuating during the cycle. Electrolyte formulations have evolved to complex mixtures containing additives conforming to SEI properties, such as lithium difluoro(oxalate)borate (LiDFOB) and lithium bis(oxalato) borate (LiBOB), which promote the formation of a stable SEI layer, and lithium nitrate ($LiNO_3$), which is known to suppress lithium dendrite growth.[12]

Open Access Article. Published on 14 juin 2024. Downloaded on 2025-01-24 19:52:32.
This article is licensed under a Creative Commons Attribution-NonCommercial 3.0 Unported Licence.

Table 1 Comparison of the cycling performance of AFLMBs with various electrolytes[a]

Current collector	Electrolyte	Cathode	Capacity	Voltage window (V)	Rate (C)	Cycle	CR (%)	CE (%)	Ref.
Cu	1 M LiDFOB + 0.2 $LiBF_4$ in FEC : DEC (1 : 2 vol.)	NMC532	2.4 mA h cm^{-2}	3.6–4.5	0.2/0.5	90	80	99.75	21
Cu	2 M LiDFOB + 1.4 $LiBF_4$ in FEC : DEC (1 : 2 vol.)	NCM532	3.1 mA h cm^{-2}	3.6–4.5	0.2/0.5	200	80	99.89	24
Cu	4 M LiFSI in DME	$LiFePO_4$	148 mA h g^{-1}	3.0–3.8	0.2/2	100	54	99.8	31
Cu	2 M $LiPF_6$ in EC : DEC (1 : 1 vol.) diluted by 50% FEC	NCM111	2 mAh cm^{-2}	2.5–4.3	0.1	50	40	97.8	30
Cu	2 M LiFSI + 1 M LiTFSI in DME/DOL (1 : 1 vol.)	$LiFePO_4$	1.6 mA h cm^{-2}	3–3.8	0.12	100	33	98.9	33
Cu	1 M $LiBF_4$ + 1 M LiDFOB in tFEP/FEC	NCM811	4.64 mA h cm^{-2}	3–4.6	0.1/0.5	100	80	98.7	36
Cu	1 M $LiPF_6$ in EC : DEC : DMC (1 : 1 : 1, vol.) with 2 wt% $LiAsF_6$ and 2 wt% FEC	NMC532	3.98 mA h cm^{-2}	3–4.3	0.125	50	75	98.3	39
Cu	1 M LiFSI in FDMB	NMC532	2.7 mA h cm^{-2}	2.7–4.3	0.1/0.3	100	80		41
Cu	ILE	NMC622	3.5 mA h cm^{-2}	1.5–4.5	0.5	100	53	99.4	45
Cu@Si-PAN	4.5 M LiFSI in $Py_{13}FSI$ with 1 wt% LiFSI	$LiNi_{0.5}Mn_{1.5}O_4$	120 mA h g^{-1}	3–4.8	0.4	120	80	99	46
Cu	1 m $LiPF_6$ + 0.5 M in FEC/DME blended with PVDF-*co*-HFP	$LiFePO_4$	1.66 mA h cm^{-2}	2.5–4	0.2	100	56.1	99.7	50
Cu	tGPE	$LiFePO_4$	1.73 mA h cm^{-2}	2.5–4	0.2	100	62.2		58
Cu	LiTFSI (80%) and $Ti_3C_2T_x$ Mxene (3 wt%) in PVDF-HFP	Li_2S@$Ti_3C_2T_x$ MXene	6.7 mA h cm^{-2}	1.7–2.8	0.33	180	84	99.9	62
LiPAA-Ag/Cu	LiC_6-coated $Li_{6.5}La_3Za_{1.5}Ta_{0.5}O_{12}$	$LiFePO_4$	0.72 mA h cm^{-2}		0.05	120	91.3	99.7	64
Cu	$Li_7La_3Zr_2O_{12}$	PEO-NCA	2.7 mA h cm^{-2}	3–4.2	0.1	50	75		65

[a] Abbreviations: CR: capacity retention; CE: coulombic efficiency; LiDFOB: lithium difluoro(oxalato)borate; $LiBF_4$: lithium tetrafluoroborate; LiFSI: lithium bis(fluorosulfonyl)imi; $LiPF_6$: lithium hexafluorophosphate; LiTFSI: lithium bis(trifluoromethanesulfonyl)imide; $LiNO_3$: lithium nitrate; $Py_{13}FSI$: *N*-methyl-*N*-propyl pyrrolidinium bis(fluorosulfonyl)imide; $LiAsF_6$: lithium hexafluoroarsenate; FEC: fluoroethylene carbonate; DEC: diethyl carbonate; EC: ethylene carbonate; DME: 1,2-dimethoxyethane; DOL: 1,3-dioxolane; DMC: dimethyl carbonate; FDMB: fluorinated 1,4-dimethoxybutane; PVDF-HFP: poly(vinylidene fluoride-*co*-hexafluoro propylene); PHEMA: poly(2-hydroxyethyl methacrylate); ILE: phosphonium bis(fluorosulfonyl)imide super-concentrated ionic liquid; tGPE: 0.5 M LiTFSI + 0.5 M $LiPF_6$ + 0.3 wt% $LiNO_3$ in DOL/DME (1 : 1 vol.) blended with PVDF-*co*-HFP and PHEMA. NMC532: $LiNi_{0.5}Mn_{0.3}Co_{0.2}O_2$; NCM111: $LiNi_{1/3}Mn_{1/3}Co_{1/3}O_2$; NCM811: $LiNi_{0.8}Mn_{0.1}Co_{0.1}O_2$; NMC622: $LiNi_{0.6}Mn_{0.2}Co_{0.2}O_2$; PEO-NCA: polyethylene oxide-$LiNi_xCo_yAl_{(1-x-y)}O_2$.

This journal is © The Royal Society of Chemistry 2024

Open Access Article. Published on 14 juin 2024. Downloaded on 2025-01-24 19:52:32.
This article is licensed under a Creative Commons Attribution-NonCommercial 3.0 Unported Licence.

2.2 The composition and function of electrolytes

One core problem of AFLMBs originates from the reactivity of electrolyte and lithium, and the goal is to create a SEI with both decent Li ion conductivity and electrical insulation. An ideal SEI should be mechanically strong yet flexible enough to withstand strains from lithium plating and stripping without cracking. In addition, a comprehensive approach to electrolyte development should be based on an understanding of not only the chemical composition but also the physical interactions at the electrode–electrolyte interface.[13] Quantitative studies have shown that the stability of the SEI is related to the lithium salt concentration of the electrolyte. For example, a high concentration of lithium hexafluorophosphate ($LiPF_6$) in a mixture of ethylene carbonate (EC) and dimethyl carbonate (DMC) has been found to improve the mechanical properties of SEIs, but it can also increase the viscosity, which may impede lithium-ion transport. Meanwhile, the introduction of dual-salt systems has been found to create a more homogeneous SEI with better mechanical integrity.[14] The recent developments in electrolytes are summarized in Table 1.

Comparatively, while solid-state electrolytes (SSEs) offer a promising path towards safer AFLMBs, their ionic conductivities are typically much lower than those of liquid electrolytes. For example, typical solid-state electrolytes can exhibit ionic conductivities in the range of 10^{-3} to 10^{-4} S cm^{-1}, which is lower than the high conductivity of 10^{-2} S cm^{-1} often found in liquid electrolytes. Strategies to improve SSE ionic conductivity include doping with heterovalent ions or creating composite electrolytes that combine polymers and ceramics to get the best of both materials. Additionally, the stability of SSEs can be determined from their electrochemical window, with many electrolytes being stable up to 5 V relative to lithium metal, while a 4 V stability limit is often observed in many liquid electrolytes. Such quantitative measures are necessary to evaluate and compare the performance, safety, and cycling stability of different electrolyte systems in AFLMBs.[15] Therefore, the scientific advancement of electrolytes for AFLMBs is a delicate balancing act between enhancing ionic conductivity and maintaining electrochemical stability. By combining experimental data and comprehensive analysis, researchers aim to develop electrolyte systems that can reliably support the high energy density and cycling stability required for next-generation battery technologies.

2.2.1 Liquid electrolytes. In the intricate system of the anode-free lithium metal battery, the electrolyte's role extends beyond mere ionic transportation—it is a vital component that significantly affects the battery's coulombic efficiency (CE) and the structural integrity of the deposited lithium on the anode CC. The corrosion between lithium and electrolyte is governed

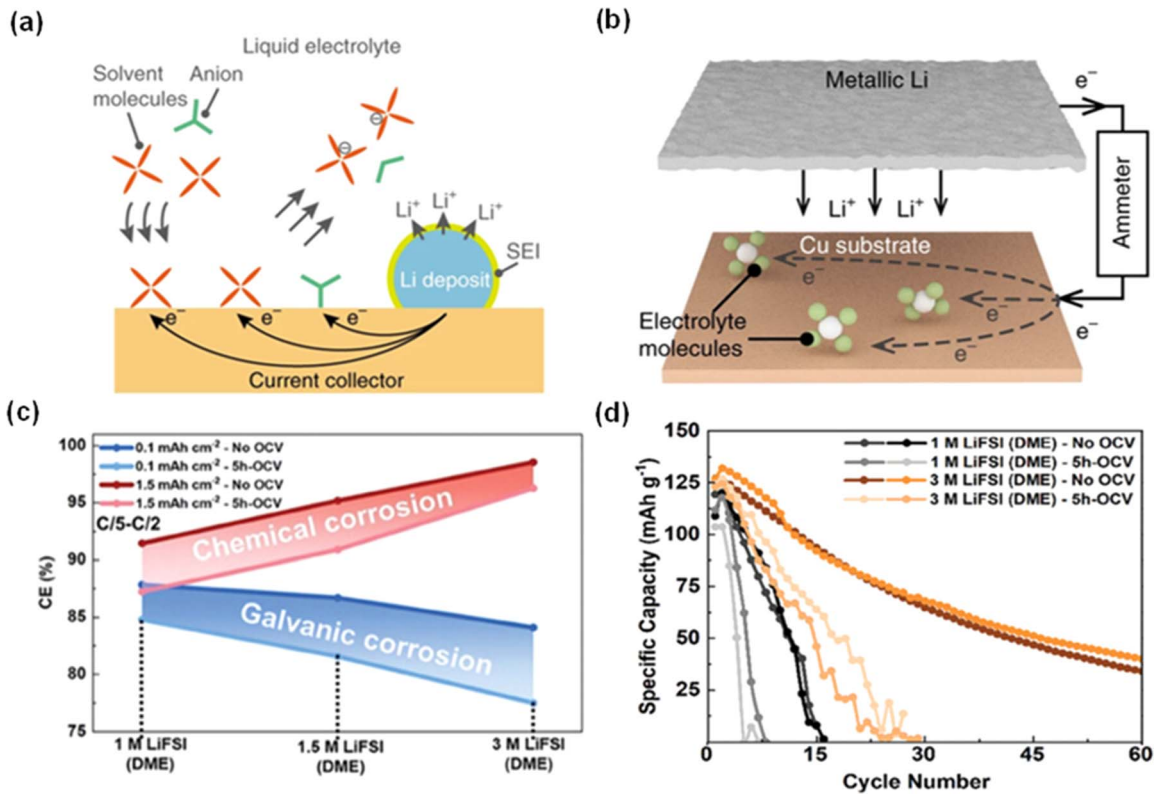

Fig. 2 Lithium galvanic corrosion and testing method. (a) The mechanism of galvanic corrosion through transporting electrons using a current collector. (b) The schematic of testing the galvanic corrosion. The current flow through an ammeter quantifies the corrosion rate of Li connected to the current collector.[16] Reproduced with permission. Copyright 2019, Springer Nature. (c) Average CEs of cells assembled with LiFSI (DME) of different concentrations and tested with a capacity of 0.1 or 1.5 mA h cm^{-2}. (d) Cycling performance of Cu||LCO employing 1 M LiFSI (DME) and 3 M LiFSI (DME) with and without a 5-hour open circuit voltage (OCV).[17] Reproduced with permission. Copyright 2023, Wiley-VCH.

Open Access Article. Published on 14 juin 2024. Downloaded on 2025-01-24 19:52:32.
This article is licensed under a Creative Commons Attribution-NonCommercial 3.0 Unported Licence.

by electrochemical processes and can be categorized into two main reactions: chemical corrosion, which stems from the direct chemical reaction between lithium and the electrolyte, and galvanic corrosion, as displayed in Fig. 2a, which involves electron transfer from lithium to the electrolyte *via* the current collector. Fig. 2b shows the schematic of a galvanic cell quantifying the corrosion rate. By applying the same potential to Li foil and a Cu substrate, the current flow recorded using an ammeter will be purely from galvanic corrosion.[16] Zhou *et al.* highlighted the influence of salt concentration and solvent choice on the corrosion behavior within AFLMBs. As demonstrated in Fig. 2c, higher salt concentrations can mitigate chemical corrosion by promoting the formation of less soluble corrosion products such as Li_2O and LiF, yet they concurrently escalate galvanic corrosion risk.[17,18] In addition, this study further confirmed that, overall, an increase in the salt concentration will generally enhance the uniformity of lithium deposition, thus improving the cycling performance (Fig. 2d).

To combat lithium corrosion, Zhou and co-workers developed a novel electrolyte consisting of 0.5 M lithium bis(-fluorosulfonyl)imide (LiFSI), 0.5 M LiDFOB, and 0.5 M $LiNO_3$ in a dimethoxyethane (DME)/fluoroethylene carbonate (FEC) mixture at a 1 : 1 volume ratio, achieving a notably low CE loss of 0.13%.[17] The effectiveness of LiDFOB has been repeatedly linked to its impact on SEI composition and the morphology of the deposited lithium.[14,19–22] In a study by Weber *et al.*, a high-performance dual-salt electrolyte blend of LiDFOB with lithium tetrafluoroborate ($LiBF_4$) in a FEC/DEC solvent mixture exhibited a capacity retention of 80% over 90 cycles for AFLMBs with $LiNi_{0.5}Mn_{0.3}Co_{0.2}O_2$ cathodes, shown in Fig. 3a.[21] However, it was noted that using LiDFOB alone could result in substantial gas generation and compromise the cut-off voltage.[23]

In addition, Louli *et al.* then conducted rigorous testing on dual-salt electrolytes with higher concentrations, specifically 2 M LiDFOB and 1.4 M lithium tetrafluoroborate ($LiBF_4$).[24] As depicted in Fig. 3b, this electrolyte extended battery life up to 200 cycles when exposed to an operating pressure of 1170 kPa. The improvement is attributed to not only the high concentration, but also the high-pressure environment which can reduce the porosity of plated lithium, effectively minimizing the depletion of the electrolyte by limiting its flow into the lithium's pores. Generally, high pressure would constrain the structure of the battery and induce a more compactly plated Li layer, which is demonstrated in Fig. 3c.[25,26]

The recent shift towards concentrated electrolytes has been catalyzed by their promising oxidative stability and high lithium-ion availability.[27–30] For example, a notable electrolyte

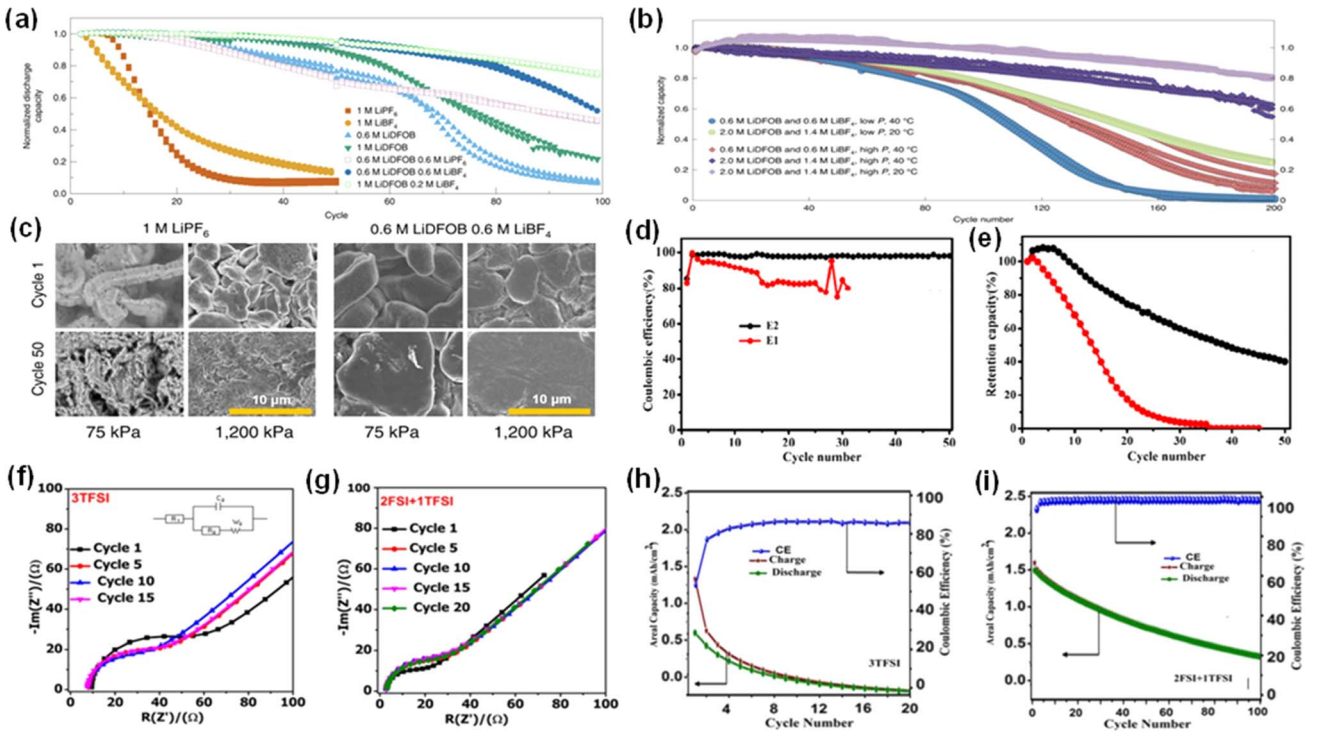

Fig. 3 Electrochemical performance of batteries with newly developed liquid electrolytes. (a) Cycling stability of cells with different ratios of electrolytes. (b) Capacity retentions of cells using different concentrations of LiDFOB and LiBF4 at various pressures and temperatures.[24] Reproduced with permission. Copyright 2020, Springer Nature. (c) SEM images of the Li layer in AFLMBs employing two different electrolytes and cycling pressures.[21] Reproduced with permission. Copyright 2019, Springer Nature. (d and e) Comparing CE and capacity retention of Cu||NMC cells employing 1 M $LiPF_6$ in EC/DEC (E1) and 2 M $LiPF_6$ in EC/DEC (E2).[30] Reproduced with permission. Copyright 2019, the American Chemical Society. (f and g) Electrochemical impedance spectroscopy comparison of AFLMBs with a 3 M LiTFSI and a dual-salt of 2 M LiFSI + 1 M LiTFSI. (h and i) Cycling performances of anode-free cells with the single salt and the dual-salt.[33] Reproduced with permission. Copyright 2019, Electrochemical Society, Inc.

 This journal is © The Royal Society of Chemistry 2024

Open Access Article. Published on 14 juin 2024. Downloaded on 2025-01-24 19:52:32.
This article is licensed under a Creative Commons Attribution-NonCommercial 3.0 Unported Licence.

containing 4 M LiFSI in DME was produced and showed excellent cycling stability. This electrolyte has been utilized to assemble copper–lithium iron phosphate (Cu||LFP) batteries with a coulombic efficiency as high as 99.8% when the battery was charged at 0.2 mA cm^{-2} and discharged at 2 mA cm^{-2} for more than 100 cycles.[31] Furthermore, Hagos *et al.* explored a locally concentrated carbonate-based electrolyte, with 2 M $LiPF_6$ in a solvent mixture of ethylene carbonate and diethyl carbonate (EC/DEC), which was diluted using 50% fluoroethylene carbonate.[30] The function of the diluent in the concentrated electrolyte is to reduce the viscosity, thus increasing the conductivity and ion mobility.[32] Finally, this strategy led to an average coulombic efficiency of 97.8% and a capacity retention of 40% over 50 charge–discharge cycles (Fig. 3d and e).[30] Beyene and colleagues also investigated the synergistic effects of concentrated dual-salt electrolytes and made a mixture of 2 M LiFSI and 1 M lithium bis(trifluoromethanesulfonyl)imide (LiTFSI) in DME/DOL solution.[33] Dual-salt electrolyte with a positive synergistic effect will lead to a higher concentration of inorganic components in the SEI. It has been demonstrated that the SEI layers of batteries cycled in dual-salt electrolytes have a high concentration of inorganic species such as LiF, Li_2O, and Li_2CO_3.[33] These inorganic components are effective in conducting lithium ions and facilitate uniform lithium deposition. Moreover, these components also possess robust mechanical properties that can withstand the volume expansion that occurs during cycling processes, thereby improving the cycling stability of the battery.[34] Conversely, SEI layers from batteries cycled in single-salt electrolyte contain a lower proportion of inorganic components and a higher concentration of organic groups such as $ROCO_2^-$, which exhibit poorer conductivity. Additionally, the electrochemical impedance spectroscopy (EIS) spectra of the cells deploying the single salt and the dual-salt were recorded and are shown in Fig. 3f and g, which indicate the role of the dual-salt in reducing interfacial resistance and improving ion transport. When applied to Cu||$LiFePO_4$ cells, this dual-salt electrolyte with a high-concentration not only achieved a much higher average coulombic efficiency (98.9%) than cells with a concentrated single salt (3 M LiTFSI) but retained more than 50% of capacity after 50 cycles (Fig. 3h and i). These results are particularly significant, considering that high-concentration electrolytes often show viscosity and wettability problems, which can lead to elevated impedance.[33,35]

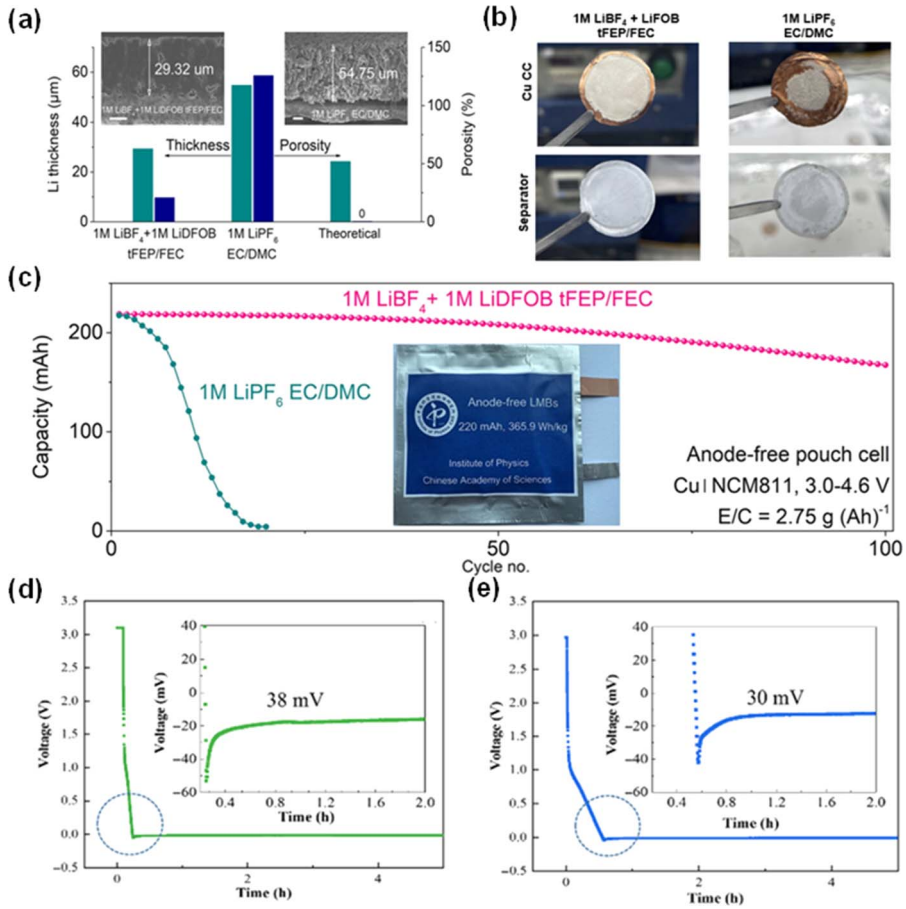

Fig. 4 The influence of porosity and dual salt on cycling stability and Li nucleation overpotential. (a) The thickness and porosity of the deposited Li layer employing a dual salt and baseline electrolyte. (b) Images of Li morphology on a Cu substrate and separator in dual-salt electrolyte and the control electrolyte. (c) Capacity *versus* the cycle number of the Cu||NCM811 pouch cell with the dual-salt electrolyte.[36] Reproduced with permission. Copyright 2023, Springer Nature. Overpotentials of Li nucleation in Li||Cu cells using $LiPF_6$ (EC/DME/DMC) (d) without additives and (e) with additives.[39] Reproduced with permission. Copyright 2023, Wiley-VCH.

Open Access Article. Published on 14 juin 2024. Downloaded on 2025-01-24 19:52:32.
This article is licensed under a Creative Commons Attribution-NonCommercial 3.0 Unported Licence.

However, the application of high-concentration electrolytes is hindered by high impedance and solvation and dissociation problems.[36,37] To mitigate these undesired effects of high-concentration electrolytes, Mao *et al.* developed an alternative electrolyte formulation comprising 1 M $LiBF_4$ and 1 M LiDFOB in a mixed solvent of fluorinated ethylene carbonate (FEC) and bis(2,2,2-trifluoroethyl) ether (tFEP). This formulation, by virtue of its weak solvating power, encourages the formation of anion-derived and inorganic-rich electrode–electrolyte interfaces, which are generally more mechanically robust and exhibit superior lithium-ion conductivity than their organic-rich counterparts. The Li deposition layers utilizing the dual-salt and control group (1 M $LiPF_6$ EC/DMC) are shown in Fig. 4a. The thinner and less porous Li layer formed in the dual-salt system compared with that in the control group indicated its stable and homogeneous Li deposition process. The reduced porosity of the deposited lithium layer in dual electrolyte systems decreases the surface exposure to liquid electrolyte, thereby mitigating additional parasitic reactions that deplete both the electrolyte and active lithium during cycling. As battery cycles increase, more pores are generated within the lithium, consuming more electrolyte. In high-energy battery applications where the amount of electrolyte is critically limited, only minimal amounts of liquid can wet the newly exposed lithium surfaces. These surfaces rapidly convert into dry SEI layers. These dry SEI layers lack pathways for ion conditions, resulting in increased internal resistance and a loss of battery capacity.[38] Therefore, it is essential to decrease the porosity of the Li deposition layer to obtain a compact and dense layer. Fig. 4b compares the Li morphology on a Cu current collector and separator with the aforementioned electrolyte and the control electrolyte (1 M $LiPF_6$ EC/DMC) after cycling, showing the firm bond between Li deposits and the Cu CC in 1 M $LiBF_4$ + 1 M LiDFOB tFEP/FEC. When the electrolyte was employed in a pouch cell with the Cu||NCM811 configuration, a high and stable cycling voltage of 4.6 V and a capacity retention of 80% were reached over 100 cycles (Fig. 4c).[36]

Recently, Wu *et al.* introduced additives (2% $LiAsF_6$ and FEC) to a $LiPF_6$-based electrolyte in an EC/DEC/DMC solvent mixture. Specifically, they examined the lithium nucleation overpotential, an important parameter of the energy required to initiate lithium deposition on a current collector.[39] The presence of additives was shown to reduce the nucleation overpotential, as evidenced by the decreased voltage gap between the initial nucleation and the growth regions, indicative of a lower energy barrier and, consequently, more uniform lithium growth.[40] As shown in Fig. 4d and e, the lower overpotential for the electrolyte with additives signifies the decreased heterogeneous nucleation barrier energy, leading to a better lithium plating surface. In this study, NMC523 was selected as the cathode and bare copper was the CC anode. 75% of the initial capacity was maintained for the cells employing the electrolyte with the dual additives after 50 cycles, and this is much higher than that of the cells using its counterpart electrolyte (without additives) which is also a recently commercialized electrolyte.

Additionally, Yu and co-workers designed a single-salt electrolyte which employed LiFSI as the solute and fluorinated 1,4-dimethoxybutane (FDMB) as the solvent. When 1 M LiFSI-FDMB was employed in Cu||NMC532 pouch cells, a capacity retention of 80% was demonstrated after 100 charge–discharge cycles. Moreover, this single-salt electrolyte exhibited a high oxidative voltage of more than 6 V.[41]

Rigorous studies were conducted to examine the effects of salt types, solvent types, salt concentrations, and additives on the electrolytic environment within AFLMBs. Each modification is thoroughly assessed for its contribution to improving the operational efficiency and longevity of AFLMBs, ensuring that the advancements in electrolyte chemistry are both firm and replicable.

2.2.2 Ionic liquid electrolytes. Ionic liquids (ILs), with their unique composition solely of cations and anions, present distinct electrochemical properties conducive to battery performance enhancements.[42] The advantages of ILs, including high ion conductivity and wide electrochemical window, have been analyzed in the context of anode-free lithium metal batteries. Their low volatility and thermal stability provide advantages over conventional liquid electrolytes in terms of stability and safety of AFLMBs.[43]

Gaetan and co-workers evaluated the performance of phosphonium bis(fluorosulfonyl)imide (FSI-) ionic liquid electrolyte (ILE). A series of characterization methods were employed to illustrate the mechanism of SEI formation in ILE, and it was found that the compounds in the SEI were mainly from the decomposition of FSI- and could provide protection for lithium (Fig. 5a).[44] Pathirana *et al.*'s pioneering work on the incorporation of bis(fluorosulfonyl)phosphonium into imide super-concentrated ionic liquid electrolyte AFLMBs is another significant paradigm.[45] They combined this ILE with a single crystal nickel manganese cobalt oxide (sc-NMC622) cathode, designing a Cu||scNMC622 cell configuration. The results are remarkable, with the battery retaining 53% of its initial capacity over 100 cycles and achieving an average coulombic efficiency (CE) of 99.4%. This study, depicted in Fig. 5b, demonstrates the potential of ILEs and shows that even when lithium decay was present, the initial stack specific energy of the AFLMB was substantially higher than that of traditional lithium-ion batteries, reaching upwards of 600 W h kg^{-1}. These data show that although CE and energy retention are promising, further research is needed on longevity and the mechanism of capacity fade during cycling. This could provide insight into the long-term stability and performance of ILE in commercial AFLMB applications.

To further investigate ILs, Liang *et al.* assessed an ionic liquid electrolyte comprising a 4.5 M LiFSI solution in *N*-methyl-*N*-propylpiperidinium bis(fluorosulfonyl)imide ($Py_{13}FSI$) with 1 wt% LiTFSI.[46] This formulation not only expanded the electrolyte's electrochemical window beyond 5 V but also facilitated the formation of a stable, fluorine-rich SEI layer. Additionally, as shown in Fig. 5c and d, ionic liquid electrolyte possesses a much higher thermal stability, indicating the improved safety of cells with ILE. In this study, the strategic addition of a silicon-polyacrylonitrile (Si-PAN) coating to the Cu current collector was designed to enhance compatibility with the IL, exploiting the synergistic effect of Si, PAN and Cu substrates to improve SEI

Open Access Article. Published on 14 juin 2024. Downloaded on 2025-01-24 19:52:32.
This article is licensed under a Creative Commons Attribution-NonCommercial 3.0 Unported Licence.

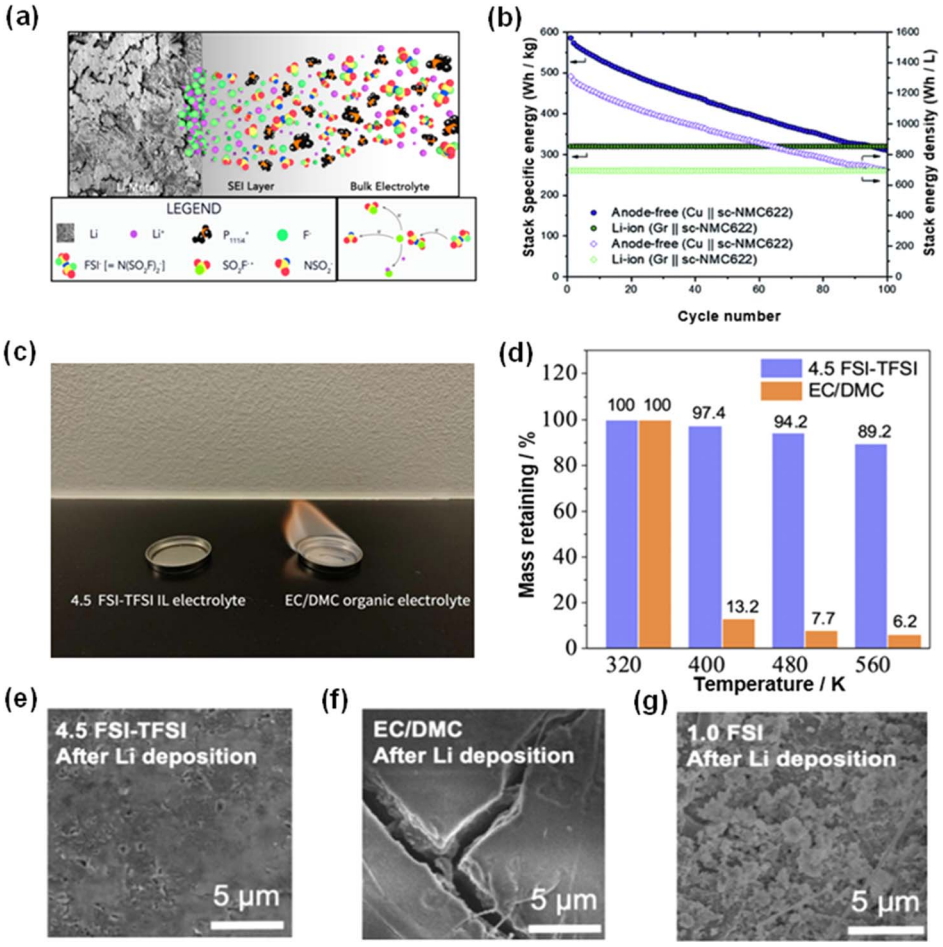

Fig. 5 Robust SEI, high thermal stability and cycling performance in an ionic-liquid electrolyte system. (a) SEI formation in ionic liquid electrolyte.[44] Reproduced with permission. Copyright 2018, the American Chemical Society. (b) Energy densities and cycling performances of the AFLMB cell and Li-ion cell employing the phosphonium-based ionic electrolyte.[45] Reproduced with permission. Copyright 2021, the Royal Society of Chemistry. (c) Flammability test of ionic liquid and electrolyte with organic solvent. (d) Thermal stability test of 4.5 FSI-TFSI ionic liquid and organic electrolyte. The morphologies of the deposited Li layer on the current collector of cells employing (e) 4.5 FSI-TFSI ILE, (f) EC/DMC and (g) 1.0 FSI IL.[46] Reproduced with permission. Copyright 2022, Wiley-VCH.

integrity and cycling performance.[47,48] The AFLMBs deploying the aforementioned ILE and modified current collector showcased a high discharge voltage of 4.7 V and retained 80% of their initial capacity following 120 cycles.[46] From the scanning electron microscopy (SEM) images provided in Fig. 5e–g, the morphological differences in lithium deposition across various electrolyte compositions show the positive effect of ionic liquid on the lithium plating process.[46] These images demonstrate the role of the ionic liquid electrolyte in determining the uniformity and density of the plated lithium, which are crucial factors for the long-term stability and performance of the AFLMB.

In conclusion, the emergence of ILs in AFLMBs represents a transformative development of electrolytes with the potential to address some long-standing problems in battery technology. However, a comprehensive and critical analysis of their long-term performance, fabrication costs and comparative results remains essential to determine their role in future applications.

2.2.3 Gel polymer electrolytes. In the dynamic environment of anode-free lithium metal batteries, the electrode will undergo large volume changes due to the cycling process of lithium plating and stripping. Conventional solid-state electrolyte interphases (SEIs), rich in lithium fluoride (LiF) and lithium oxide (Li_2O), while mechanically sound, often fail to adapt to these changes, leading to rigidity-induced failure and continuous lithium loss.[49] To provide SEIs with the necessary flexibility and robustness, researchers have pivoted towards gel polymer electrolytes (GPEs) and have amalgamated polymers into liquid electrolytes to impart the necessary mechanical flexibility and robustness to SEIs. These hybrid electrolytes demonstrate excellent electrode–electrolyte interfacial contact and reduced electrical impedance compared with pure solid-state electrolytes, which are also essential factors in maintaining the integrity and functionality of AFLMBs throughout their lifespan.[50–52]

Polyvinylidene fluoride–hexafluoropropylene copolymer (PVDF-*co*-HFP), known for its semi-crystalline structure, has emerged as a formidable component in the construction of GPEs due to its ability to provide solvent stability and

Open Access Article. Published on 14 juin 2024. Downloaded on 2025-01-24 19:52:32.
This article is licensed under a Creative Commons Attribution-NonCommercial 3.0 Unported Licence.

mechanical support in the electrolyte matrix.[53] Although its application in AFLMBs has been documented, predominantly in the context of the production of artificial SEIs under strict laboratory conditions, the full potential of PVDF-*co*-HFP in practical batteries remains to be investigated in detail.[54–56]

Lin *et al.* advanced this field by fabricating a GPE (FN-GPE) composed of PVDF-*co*-HFP, lithium hexafluorophosphate ($LiPF_6$), and lithium nitrate ($LiNO_3$) in a binary solvent system of fluoroethylene carbonate (FEC) and dimethoxyethane (DME).[50] This GPE was compared with various $LiPF_6$ and $LiNO_3$ concentrations in FEC-DME (F-LE and FN-LE) to assess the impact of the polymer on lithium deposition morphology. As shown in Fig. 6a, the SEI formed in the FN-GPE system has a higher content of Li_3N and Li_2O, which indicates the enhanced Li ion conductivity in the layer. Additionally, Fig. 6b illustrates the electrostatic potential of organic solvents and PVDF-*co*-HFP, and it has been concluded that the positive region (deep blue) of PVDF-*co*-HFP will bond with negative ions, thus improving Li^+ transfer efficiency. Scanning electron microscopy shows that FN-GPE can induce a denser lithium layer with a minimum thickness, suggesting a homogeneous plating process. Atomic force microscopy (AFM) studies also confirmed the mechanical elasticity of the SEI layer formed in GPE, which displayed a notable elasticity and resistance to structural collapse.[50]

The incorporation of poly(2-hydroxyethyl methacrylate) (PHEMA) into the GPE framework of PVDF-*co*-HFP presents a strategic advancement.[57,58] The polar side chains of PHEMA enhance the regulation of lithium ion flow, promoting the formation of compact lithium deposition. A ternary-salt GPE (tGPE) with a blend of PHEMA and PVDF-*co*-HFP developed by Lin's team, integrating LiTFSI and $LiPF_6$ with a minor

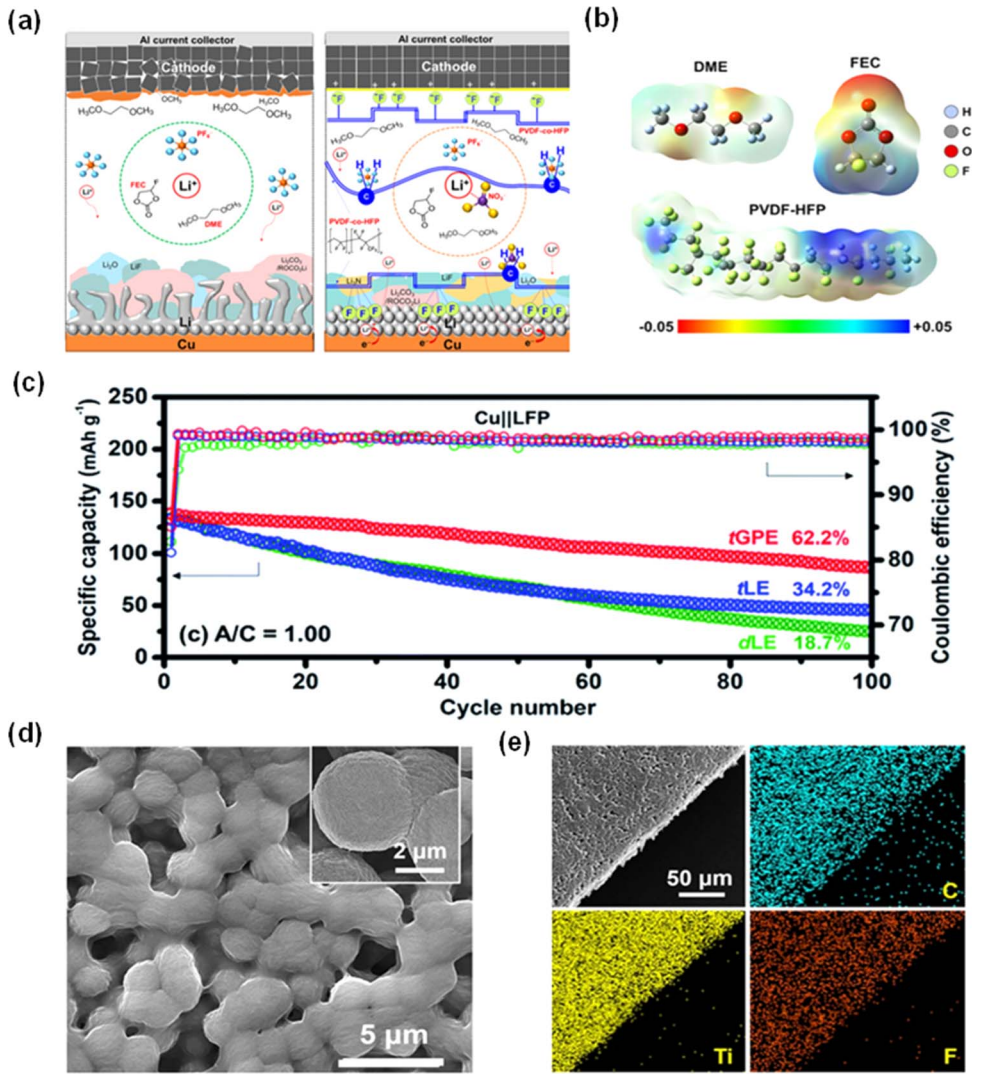

Fig. 6 Electrochemical performance of gel polymer electrolytes. (a) Impact of FN-FPE electrolyte on electrochemical performance of batteries. (b) Illustration of the electrostatic potential surface of different electrolytes.[50] Reproduced with permission. Copyright 2023, Elsevier. (c) Cycling performance of Cu||LFP cells employing tGPE, tLE and dLE.[58] Reproduced with permission. Copyright 2022, the Royal Society of Chemistry. (d) SEM image of composite gel polymer electrolyte (CGPE). (e) EDS images of elements in CGPE.[62] Reproduced with permission. Copyright 2022, Springer Nature.

 This journal is © The Royal Society of Chemistry 2024

Open Access Article. Published on 14 juin 2024. Downloaded on 2025-01-24 19:52:32.
This article is licensed under a Creative Commons Attribution-NonCommercial 3.0 Unported Licence.

proportion of $LiNO_3$ in DOL-DME, showcased improved ionic conductivity and fostered the development of a durable, lithium fluoride-rich SEI.[58] Although $LiPF_6$ may undergo undesired reactions in ether-based solvents because the PF_5 from the decomposition of $LiPF_6$ can trigger the polymerization of DOL, the presence of $LiNO_3$ will curtail such side reactions, enabling a stable electrolyte system.[58–61] The Cu|tG-PE|LFP AFLMBs utilizing this electrolyte formulation displayed a commendable capacity retention of over 62% after 100 cycles of charge–discharge cycles at 1 mA cm^{-2} current density (Fig. 6c). In addition, Liu and co-workers developed a composite gel polymer electrolyte (CGPE) composed of LiTFSI in PVDF–HFP and $Ti_3C_2T_x$ MXene. As shown in Fig. 6d and e, the resulting CGPE has a porous structure, which not only enjoys excellent Li ion conductivity but also offers a satisfactory mechanical strength.[62]

These studies emphasize the crucial role that polymers play in enhancing the mechanical and electrochemical performance of SEIs within AFLMBs. The combined experimental evidence from SEM and AFM analyses provides a convincing narrative for the adoption of GPEs in AFLMBs, marrying mechanical flexibility with electrochemical efficiency. It is clear that the future of AFLMB electrolyte development will hinge on a balance of polymer chemistry and electrolyte formulation to optimize both the mechanical integrity and ionic transport within the battery architecture.

2.2.4 Solid-state electrolytes. Solid-state electrolytes (SSEs) are at the cutting edge of anode-free lithium metal battery innovation, providing a revolutionary change towards batteries that are not only durable and safe, but can reduce the likelihood of leakage and flammability problems associated with liquid electrolytes. However, the development of solid electrolyte in the application of AFLMBs also faces severe challenges. A key issue is the creation of robust interfacial contact between the solid-state electrolyte and electrodes. This interface is critical as it dictates the ion transfer efficiency which in turn affects the overall battery performance. Poor interfacial contact results in high resistance to ion flow, leading to inefficiencies that can manifest as reduced power output and increased charge times. Lee *et al.* reported a Ag–C composite layer (Fig. 7a), which can effectively regulate Li deposition and thus lead to uniform and dendrite-free Li plating.[63] As a result, lithium metal pouch cells assembled with the layer and Li_6PS_5Cl SSE achieved high energy density (>900 W h L^{-1}) and long cycle life (1000 cycles). Similarly, Huang *et al.* designed multi-functional layers to achieve long-term operation in terms of the garnet-based solid-state AFLMB (Fig. 7b). The multi-functional layers include a LiC_6 layer with high Li ion conductivity, a ductile lithiated polyacrylic acid polymer layer with interfacial self-adaption ability and a Ag nanoparticles layer with regulated Li deposition.[64]

Another significant challenge is the inherently lower ionic conductivity of SSEs compared to liquid electrolytes, which

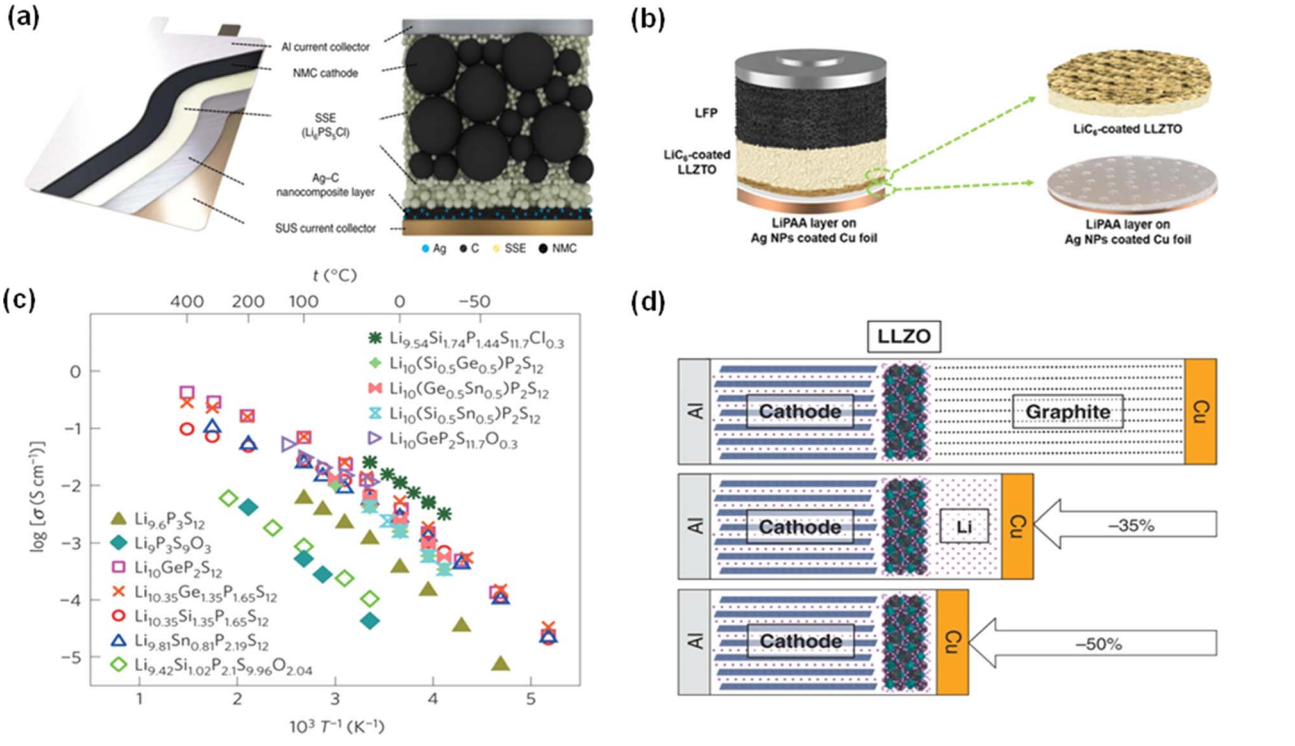

Fig. 7 Recent designs of solid-state electrolytes. (a) Schematic of an all-solid-state battery composed of a NMC cathode, SSE and a Ag–C nanocomposite anode layer.[63] Reproduced with permission. Copyright 2020, Springer Nature. (b) Schematic of a garnet-based anode-free cell.[64] Reproduced with permission. Copyright 2020, Wiley-VCH. (c) Arrhenius conductivity plots for the sulfide electrolyte family $Li_{9.6}P_3S_{12}$ and $Li_{9.54}Si_{1.74}P_{1.44}S_{11.7}Cl_{0.3}$.[67] Reproduced with permission. Copyright 2026, Springer Nature. (d) Comparison of the solid-state Li metal battery, solid-state Li ion battery and solid-state anode-free battery.[65] Reproduced with permission. Copyright 2020, Springer Nature.

Open Access Article. Published on 14 juin 2024. Downloaded on 2025-01-24 19:52:32.
This article is licensed under a Creative Commons Attribution-NonCommercial 3.0 Unported Licence.

requires advanced material engineering to create ion pathways that are both conductive and stable.[60,65] Generally, sulfide electrolyte shows a high ionic conductivity of $>10^{-3}$ S cm^{-1} and is regarded as a kind of promising SSE.[66] Kanno *et al.* reported a lithium superionic conductor containing sulfide with high ionic conductivity (25 mS cm^{-1}) and high stability (~0 V *vs.* Li metal).[67] In addition, oxide electrolytes are also promising because they show higher electrochemical stability and less reactivity towards lithium.[68] Wang *et al.* showed the potential for AFLMBs using $Li_7La_3Zr_2O_{12}$ (LLZO) electrolytes, and the fabricated battery only has a much smaller volume, shown in Fig. 7d, around half of the corresponding Li ion battery.[65] A full cell consisting of *in situ* formed Li, LLZO and NCA showed a high capacity retention of 75% after 50 cycles.

Moreover, the complexity of fabricating SSEs with precise structural and compositional integrity surpasses that of synthesizing liquid electrolytes, representing another layer of complexity in the mass production of AFLMBs with SSEs. This is compounded by the necessity for strict control over the manufacturing environment to prevent contamination and ensure consistency. Despite these challenges, the promise of solid electrolytes is too significant to ignore. They are expected to play an important role in the development of next-generation AFLMBs, particularly in applications where safety is paramount. As the field evolves, the focus remains on overcoming the challenges inherent to solid-state electrolytes, with the ultimate goal of delivering batteries that offer not just improved safety, but also superior energy density, longevity, and reliability.

3. Development of current collectors towards homogeneity of lithium deposition

3.1 Copper current collector

Copper's role as a current collector is essential in lithium-based batteries, valued for its high conductivity and stability. However, its tendency to promote unregulated lithium deposition causes serious problems such as dendrite and loose lithium layers, shown in Fig. 8a, affecting the performance and safety of the battery. To combat this, surface modification techniques are significant.[69] By alloying copper with metals that have a high affinity for lithium, applying conductive coatings, and creating micro- or nano-scale structures, a lithiophilic surface can be cultivated to encourage uniform lithium nucleation and growth. The mechanism of the lithiophilic surface is shown in Fig. 8b.[70,71] In addition, the development of other types of current collectors, such as carbon and zinc, is also increasing. A summary of recent current collector modification strategies is shown in Table 2.

3.1.1 Metal coatings. The adoption of prelithiation techniques has emerged as a means to counteract copper's poor lithiophilicity. By infilling grain boundaries of a current collector with lithium, a more uniform deposition landscape can be created. Huang *et al.* found that during the Li deposition process, Li ions can diffuse into grain boundaries of Cu, resulting in the formation of nanoscale Li on the Cu CC and uneven Li coating on the CC surface.[72] Therefore, they prelithiated the Cu CC to fill up the inside nanogap and successfully improved the Li nucleation on the Cu CC (Fig. 9a). Besides, researchers conducted other methods, such as introducing lithiophilic elements to current collectors. At the beginning, the lithium nucleation overpotential is reduced by adding inert and conductive metals (such as gold and silver) to the copper CC because the energy required for the lithium nucleation on lithiated gold or silver is very small.[73,74] However, such methods are not without trade-offs. For example, metals such as gold and silver, while initially reducing nucleation overpotential, may ultimately dissolve into Li metal and lead to the disintegration of these conductive aids and the subsequent collapse of the battery's architecture. Therefore, more stable methods to fabricate Cu CCs with other metals that are insoluble or slightly soluble in Li have been investigated.[7,75–77]

Advancements in copper surface treatment, such as tin (Sn) coatings *via* magnetron sputtering, have achieved considerable success. The formation of a Li–Sn alloy during the initial lithium depositing process drastically lowers the nucleation barrier. Recently, Wang *et al.* tested a Sn-coated Cu CC *via* magnetron sputtering (Cu/S–Sn).[7] Their design relies on the formation of the Li–Sn alloy ($Li_{22}Sn_5$) in the first lithium plating process (Fig. 9c and d), which largely increases the affinity of the current collector for lithium. It is worth noting that the Li–Sn alloy will be stable and the Li in the alloy will not be used in the following cycles. Moreover, as shown in Fig. 9b, the Li deposition layer on the modified Cu/S–Sn CC is much more stable.

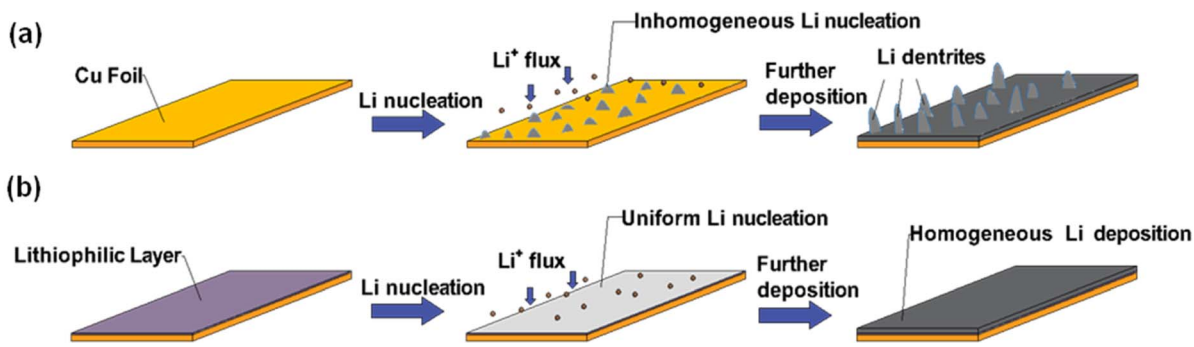

Fig. 8 Schematic diagrams of Li nucleation and growth on (a) bare Cu and (b) Cu with a lithiophilic layer.

 This journal is © The Royal Society of Chemistry 2024

Open Access Article. Published on 14 juin 2024. Downloaded on 2025-01-24 19:52:32.
This article is licensed under a Creative Commons Attribution-NonCommercial 3.0 Unported Licence.

Table 2 Summary of the cycling performance of AFLMBs with different current collector modification strategies[a]

Current collector	Electrolyte	Cathode	Capacity	Voltage window (V)	Rate (C)	Cycle	CR (%)	CE (%)	Ref.
Cu/S–Sn	1 M $LiPF_6$ in EC : DEC (1 : 1 vol.) with 5 wt% FEC	LRM	201.2 mA h g^{-1}	2–4.8	0.2	20	89	99.4	7
E-Cu	6 M LiFSI in DME	NCM811	200 mA h g^{-1}	2.2–4.3	0.2	50	84	99.65	75
$LiSn_{4.4}$@Cu	6 M LiFSI in DME	NCM811	4 mA h cm^{-2}	3–4.3	0.3	50	85.5	99	78
H–Cu	6 M LiFSI in DME	NCM523	3 mA h cm^{-2}	3–4.35	0.5	100	41	99.24	82
Zn_3N_2@Cu	1 M LiFSI in DOL/DME (1 : 1 vol.) with 1 wt% $LiNO_3$	$LiFePO_4$	155 mA h g^{-1}	2.5–4	0.5	100	63.1	98.8	83
Cu@PEO	1 M LiTFSI in DOL/DME (1 : 1 vol.) with 2 wt% $LiNO_3$	$LiFePO_4$	127 mA h g^{-1}	3–3.8	0.2	200	30	98.6	85
Zn-NC-CNT-Cu	1 M $LiPF_6$ in EC : DEC : EMC (1 : 1 : 1 vol.)	NMC811	1 mA h cm^{-2}	3–4.3	0.5	50		99.5	86
ULL@Cu	1 M PF_6 in EC : DEC (1 : 1 vol.)	$LiCO_2$	172 mA h g^{-1}	3–4.3	0.5	50	98.5		87
Au@3D-Cu	2 M LiTFSI in DOL/DME with 2 wt% $LiNO_3$	$LiFePO_4$	128 mA h g^{-1}	3–3.8	0.1	100	45	98.9	89
a-RF@3D-CM	1 M LiTFSI in DOL/DME with 2 wt% $LiNO_3$	$LiFePO_4$	131.2 mA h g^{-1}	3–3.8	0.2/0.3	100	60.66	99.5	90
d-CP	1 M LiTFSI in DOL/DME with 10% FEC and 1% VC	NCM811	4.2 mA h cm^{-2}	2.7–4.3	0.48	50	90		91
Zn–N-CNF	1 M LiTFSI in DME	$LiFePO_4$	2.05 mA h cm^{-2}	2.4–4	0.5	120	91		70
PI@Au	1 M $LiPF_6$ in EC/DEC with 10% FEC and 1% VC	NCM811	6.4 mA h cm^{-2}	3–4.3	0.2	100	86		93

[a] Abbreviations: Cu/S–Sn: Sn nanolayer coated Cu foil; E-Cu: epitaxial induced plating current-collector; $LiSn_{4.4}$@Cu: $Li_{4.4}Sn$ coated Cu foil; H–Cu: cuprite nanoparticle modified Cu foil; Zn_3N_2@Cu: Zn_3N_2 layer coated Cu foil; Cu@PEO: polyethylene oxide coated Cu foil; Zn-NC-CNT-Cu: Zn-doped N-doped carbon sheet-carbon nanotube modified Cu foil; ULL@Cu: ultrathin lithiatable layer modified copper; Au@3D-Cu: Au predeposited Cu mesh; a-RF@3D-CM: resorcinol formaldehyde on 3D engineered copper mesh; d-CP: defective carbon paper; Zn–N-CNF: Zn–N_x-modified carbon nanofiber; PI@Au: Au-decorated insulating polyimide; LRM: Li rich Mn-based cathode.

Open Access Article. Published on 14 juin 2024. Downloaded on 2025-01-24 19:52:32.
This article is licensed under a Creative Commons Attribution-NonCommercial 3.0 Unported Licence.

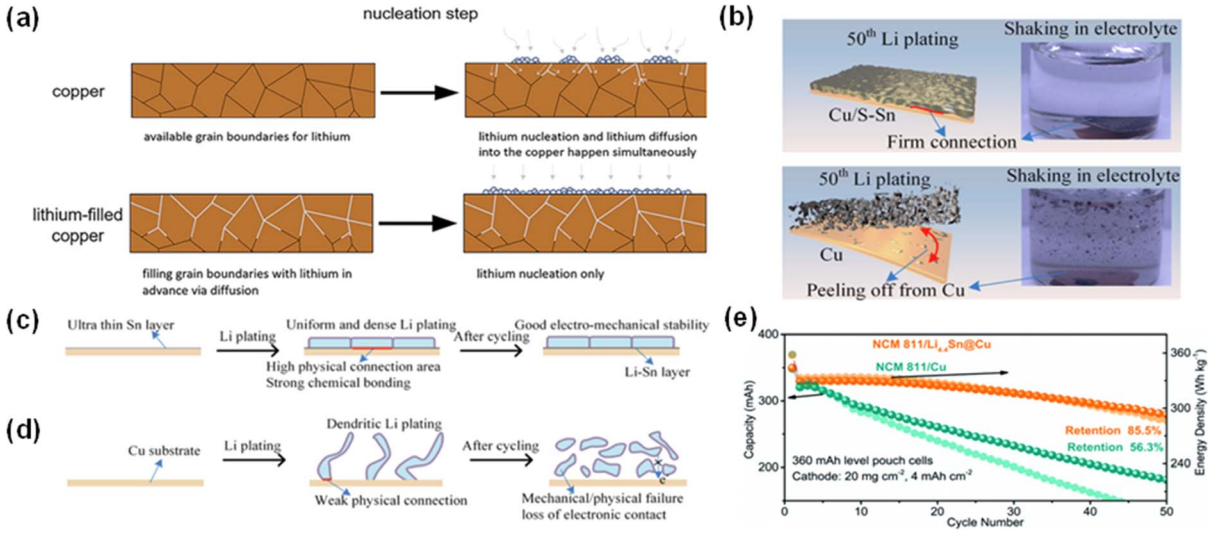

Fig. 9 Lithium nucleation and the effect of metal coatings. (a) Illustrative diagrams showcasing lithium nucleation on bare copper and pre-lithiated copper.[72] Reproduced with permission. Copyright 2023, Wiley-VCH. (b) Bonding strength testing for the Li deposition layer on Cu/S–Sn and bare Cu. The Li plating process on (c) Cu@Sn and (d) bare Cu.[7] Reproduced with permission. Copyright 2022, Elsevier. (e) Cycling stability of pouch cells of NCM811||Cu and NCM811||$Li_{4.4}Sn$@Cu.[78] Reproduced with permission. Copyright 2022, the Royal Society of Chemistry.

After 50 charge–discharge cycles, the Li plated on Cu/S–Sn still stuck to the CC while Li deposited on bare Cu dispersed heavily in the electrolyte under mechanical shaking. The obtained Cu/S–Sn CC with a carbonate-based electrolyte and lithium-rich manganese-based cathode system showed good electrochemical stability (average CE 94.1%) for 400 cycles at a current density of 1 mA cm^{-2}. Lin *et al.* developed a Cu CC with a liquid metal (LM) layer composed of Ga, In, and Sn, which also relies on the alloying reaction with Li to reduce the energy barrier.[75] The GaInSn@Cu||NCM 811 pouch cell delivered a capacity of 150 mA h cm^{-2} with a decent retention of 84% after 50 cycles.

Zhang *et al.* prelithiated Sn@Cu and obtained a $Li_{4.4}Sn$@Cu current collector.[78] They compared the electrical conductivity (EC) of $Li_{4.4}Sn$@Cu and Cu foil by AFM and found that the EC of Cu foil is even less than that of $Li_{4.4}Sn$@Cu. This is because some regions of Cu foil have higher EC while other regions possess lower EC, which will result in concentrated charge and inducing excess Li deposition in certain areas. The pouch cells deploying the modified CC and NCM811 cathode showed a capacity retention of 85.5% after cycling 50 times with an areal capacity of 4 mA h cm^{-2} (Fig. 9e).

3.1.2 Metallic compound coatings. The strategic integration of metallic compounds in anode-free lithium metal batteries marks a remarkable shift from conventional materials to more lithiophilic alternatives. For example, the deployment of zinc-based compounds in existing products presents a critical development. This material can form a homogeneous lithium–zinc (Li–Zn) alloy when lithium is deposited, making the lithium layer ordered and potentially curbing the notorious issue of dendritic growth.[79] Lithium compounds, such as LiF or Li_3N, will also be formed during cycling by utilizing the anions from metallic compounds. These lithium compounds are known for their high lithium-ion conductivity and are indicative of more stable lithium deposition—a cornerstone for durable and safe battery operation.

The trend of employing metallic compounds such as aluminum fluoride (AlF_3), zinc oxide (ZnO), and titanium carbide (TiC) is not an arbitrary choice.[71,80,81] Their lithiophilic nature leads to a deliberate goal: to reduce lithium nucleation energy, thus promoting a more efficient lithium plating process. The effect is significant, as the current collectors can not only support the quality of lithium plating but also extend battery life by exhibiting high reliability and electrochemical stability. Additionally, Xia *et al.*'s work on depositing cuprite nanoparticles on the surface of copper current collectors (HCu) by a simple atmospheric heating process points to a practical and cost-effective way to improve the electrochemical performance of AFLMBs.[82] During cycling, the HCu will react with Li ions and produce Cu nanoparticles and Li_2O. The formed nanoparticles increase the specific surface area of the current collector (Fig. 10c), thus providing more Li plating sites and inducing a smooth Li plating layer (Fig. 10a). Li_2O is produced as an artificial SEI, which could facilitate Li ion transport and enhance the electrode kinetics of the CC. A battery utilizing this novel approach achieved a capacity retention of 41% after 100 cycles at 0.5C (Fig. 10b) when the modified Cu CC was coupled with NCM523, indicating a significant enhancement in electrode kinetics.

A critical examination of Zhu's modification of a copper current collector with a zinc nitride (Zn_3N_2) film highlights the feasibility of application for these metallic compounds.[83] The relatively low nucleation overpotential on Zn_3N_2@Cu shown in Fig. 10d and e demonstrates the lithiophilic properties of the fabricated layer, thus stabilizing the Li nucleation process on the modified CC. This study demonstrated a reduction in dendrite growth, a persistent problem that affects cell integrity and function. The zinc nitride film has two functions. It actively interacts with lithium ions to form a Li–Zn alloy, which helps promote uniform lithium plating, and it helps form Li_3N

 This journal is © The Royal Society of Chemistry 2024

Open Access Article. Published on 14 juin 2024. Downloaded on 2025-01-24 19:52:32.
This article is licensed under a Creative Commons Attribution-NonCommercial 3.0 Unported Licence.

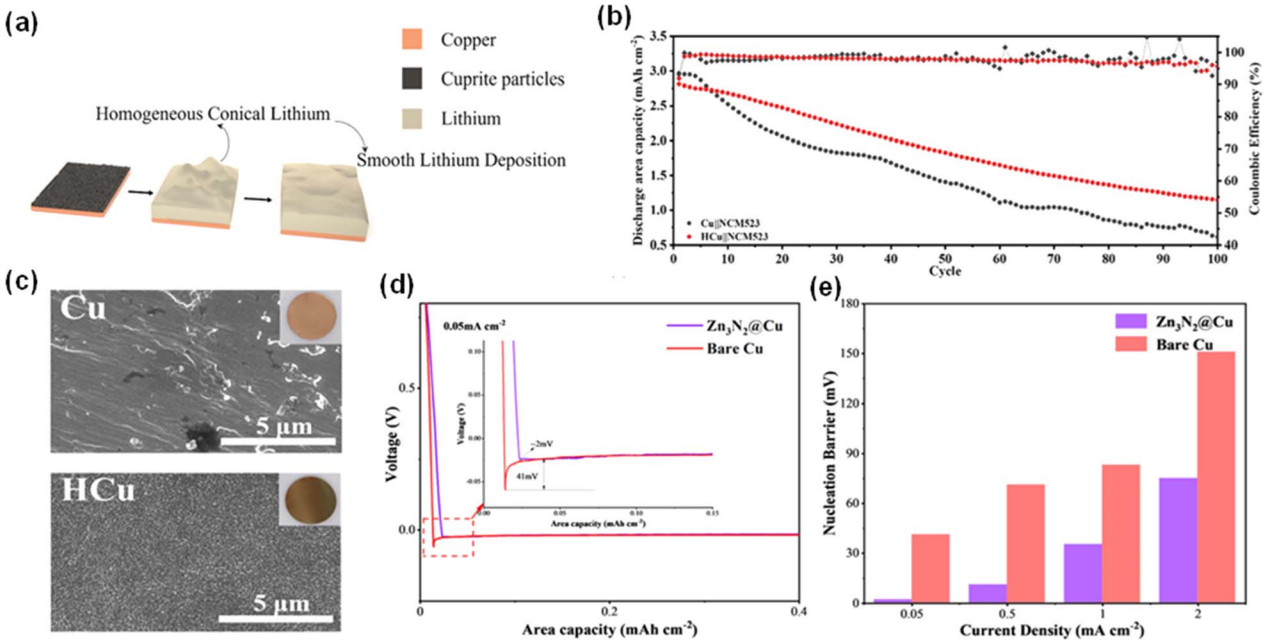

Fig. 10 Metal compound coatings on a copper current collector with their unique performance. (a) Homogeneous conical lithium deposition on the Cu CC with cuprite nanoparticles. (b) Cycling performance of Cu||NCM23 and HCu||NCM523. Reproduced with permission. (c) SEM images of the Cu current collector and heated-Cu current collector (HCu) and the insets show the optical images.[82] Copyright 2023, Elsevier. (d) Li nucleation overpotential on bare Cu and modified Cu. (e) Nucleation barrier *versus* current density for bare Cu and modified Cu.[83] Reproduced with permission. Copyright 2023, the American Chemical Society.

compounds during deposition. The presence of Li_3N is particularly important due to its high lithium-ion conductivity, which is necessary for efficient and stable lithium deposition. Full cells incorporating Zn_3N_2@Cu with lithium iron phosphate (LFP) cathodes exhibited a commendable capacity retention of 63.1% over 100 cycles and an average CE of 98.8%. Besides, it has been shown that the utilization of metallic compounds will increase the inorganic content in the SEI, suggesting the formation of a more robust and stable interphase. Therefore, the battery industry is systematically unraveling the complexity of lithium deposition through rigorous analysis of the interaction between lithium and metal compounds.

3.1.3 Other novel coatings for current collectors. In recent years, the application of polymer coating on existing materials has become an effective way to improve the stability and performance of the solid electrolyte interface (SEI) in lithium metal batteries. This advancement has great potential to solve SEI degradation, a long-standing problem in anode-free lithium metal batteries. In particular, polymer systems such as polyethylene oxide (PEO) and polyvinylidene fluoride (PVDF) have been used to form protective layers on current collectors, effectively redistributing lithium ions during coating and minimizing direct contact with electrolytes. Tamwattana *et al.* synthesized a LiF@PVDF coating with a high dielectric constant for a Cu current collector.[84] The high dielectric coating will provide a dipolar layer, guiding a more uniform Li^+ flux, thus suppressing the Li dendrite growth (Fig. 11a). Additionally, the impedance spectra in Fig. 11b show that the high dielectric LiF@PVDF layer enjoys a smaller charge transfer resistance compared with pure PVDF. Similarly, Assegie *et al.* coated a polyethylene oxide film on copper current collectors (Cu@PEO), providing a homogeneous flux of lithium ions and shielding deposited lithium from electrolytes, thereby promoting the formation of a thin and robust SEI.[85] Full cells incorporating the Cu@PEO anode CC with an LFP cathode demonstrated an average CE close to 100% over 200 cycles at 0.5 mA cm^{-2}.

Moreover, Zhao *et al.*'s innovation involving zinc-doped nitrogen–carbon structures interlaced with carbon nanotubes coated on a Cu substrate (Zn-NC-CNT-Cu) has introduced another research shift in current collector fabrication. A drastically low nucleation overpotential (4.2 mV) was observed with these coated copper foil pieces and this is because of the homogeneous distribution of lithiophilic Zn on the Cu CC, as depicted in Fig. 11c, which will then induce uniform Li deposition. Besides, at both current densities of 1 mA cm^{-2} and 2 mA cm^{-2}, cells fabricated with Zn-NC-CNT-Cu always exhibited higher CEs (Fig. 11d).[86] Recently, Kim J. *et al.*'s ultrathin lithiatable layer (ULL) application demonstrated a lower charge transfer resistance and a richer Li_2O SEI composition compared to traditional copper current collectors. In Fig. 11e, the blue layer after partial lithiation suggested that the ULL reacted with lithium, forming a layer with a higher Li affinity. The full cell with ULL@Cu led to a marked increase in capacity retention up to 98.5% over 50 cycles (Fig. 11f).[87]

These developments represent a revolutionary framework for current collector functionality in AFLMBs. Each novel coating and process will be evaluated not only for its immediate impact on electrochemical performance, but also for its long-term impact on battery life and safety. The synergistic combination

Open Access Article. Published on 14 juin 2024. Downloaded on 2025-01-24 19:52:32.
This article is licensed under a Creative Commons Attribution-NonCommercial 3.0 Unported Licence.

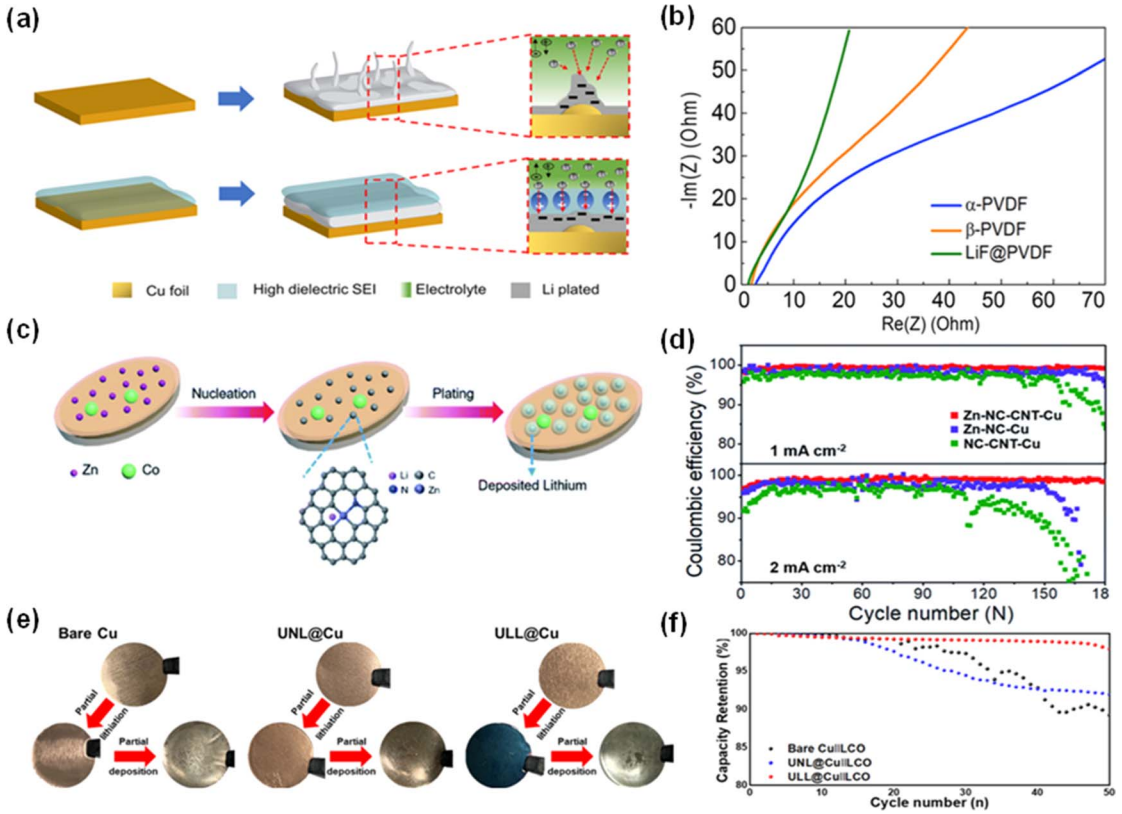

Fig. 11 Recent designs of current collector coatings. (a) Schematic of Li dendrite growth and Li dendrite suppression from a high dielectric coating. (b) Comparison of impedances in α-PVDF, β-PVDF, and LiF@PVDF.[84] Reproduced with permission. Copyright 2021, the American Chemical Society. (c) Schematic of Li nucleation and plating on a Zn-NC-CNT-Cu substrate. (d) Coulombic efficiencies *versus* cycle numbers in three different systems at 1 mA cm^{-2} and 2 mA cm^{-2}.[86] Reproduced with permission. Copyright 2021, the American Chemical Society. (e) Photographs of Li deposition on a bare Cu CC, ultrathin non-lithiatable layer (UNL)@Cu CC and ULL@Cu CC. (f) Cycling Performance of cells with the bare Cu CC and modified Cu CC.[87] Reproduced with permission. Copyright 2023, Elsevier.

of advanced coatings and innovative current collector engineering holds great promise for the future of lithium metal batteries, paving the way for enhanced performance in energy storage systems.

3.2 Three-dimensional current collectors

The evolution towards three-dimensional (3D) current collectors in AFLMBs represents a fundamental breakthrough in tackling the formidable challenges linked with volume expansion and charge distribution. Engineered to accommodate the significant volume fluctuations between lithium plating and stripping, 3D current collectors exhibit a larger surface area, fostering a more uniform distribution of charge—a critical factor for both mechanical and electrochemical stability within batteries.

Recent studies comparing 2D and 3D collectors have unveiled the potential of the latter to mitigate concentrated charge flux, thus reducing the likelihood of non-uniform lithium plating. Despite these encouraging findings, ensuring consistent high lithiophilicity across the intricate structures of 3D collectors is still a persistent challenge. Through an insightful analysis of the correlation between surface area of 3D Cu current collectors and dead lithium, Adhitama *et al.* elucidated the relationship between surface area and charge flux concentration, underlining the potential of larger surface areas to alleviate inhomogeneous lithium plating.[88] They compared three types of Cu current collectors (Fig. 12a) and found that the modified 3D Cu CC with a high-depth microstructure or large surface area can induce better electrochemical properties, displayed in Fig. 12b and c. Nevertheless, despite the increased nucleation sites, the problem of low lithiophilicity of Cu persists in current 3D collectors.

Kim *et al.* conducted a comprehensive investigation into the effects of 3D current collectors, comparing the performance of 2D Cu current collectors (Cu foil) against 3D Cu current collectors (Cu mesh) and their counterparts predeposited with Au on the surface (Fig. 12d). Fig. 12e illustrates the Li nucleation overpotentials on the four different CCs and it has been found that Au@3D Cu has the smallest value (6.5 mV) among the various CCs. Their research demonstrated that Au@3D Cu current batteries incorporated with a LFP cathode achieved a critical capacity of 45% after 100 cycles, as shown in Fig. 12f, and an average coulombic efficiency as high as 98.9%.[89] In addition, even after 100 cycles, the morphology of the Au@3D

 This journal is © The Royal Society of Chemistry 2024

Open Access Article. Published on 14 juin 2024. Downloaded on 2025-01-24 19:52:32.
This article is licensed under a Creative Commons Attribution-NonCommercial 3.0 Unported Licence.

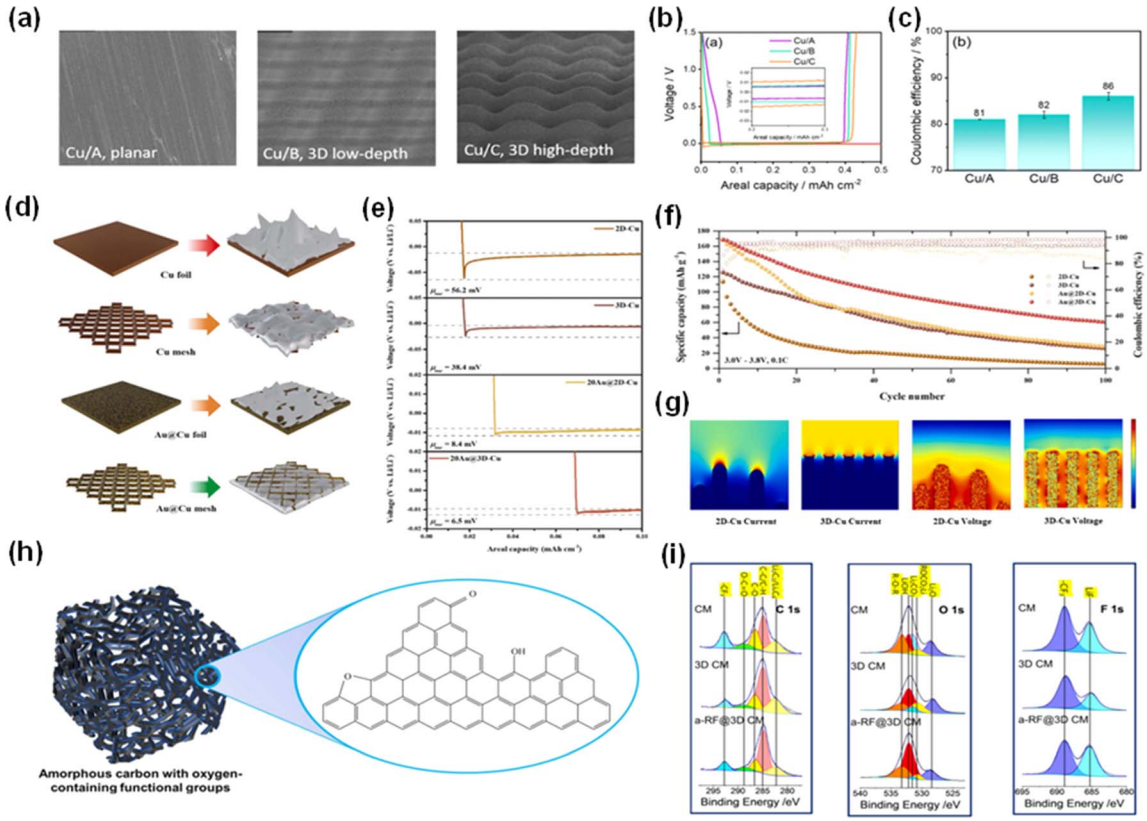

Fig. 12 3D current collectors of AFLMBs and their effects on overpotential and other performances. (a) SEM images of the planer Cu CC (Cu/A) and 3D Cu CC with low-depth (Cu/B) and high-depth (Cu/C) channels. (b) Voltage *versus* areal capacity of Li cycling of the three Cu CCs (Cu/A, Cu/B and Cu/C). (c) The coulombic efficiency during the first cycle of the cells assembled with the three Cu CCs.[88] Reproduced with permission. Copyright 2023, the Royal Society of Chemistry. (d) Schematics of 2D-Cu (foil), 3D-Cu (mesh), Au@2D-Cu, Au@3D-Cu. (e) Overpotentials measured at 50 μA cm^{-2} of the four CCs. (f) Cycling performance of the cells employing 2D-Cu, 3D-Cu, Au@2D-Cu, Au@3D-Cu. (g) Current flux and voltage distribution of 2D-Cu and 3D-Cu shown using COMSOL.[89] Reproduced with permission. Copyright 2023, Elsevier. (h) The structure of amorphous carbon transformed from resorcinol formaldehyde (RF). (i) XPS images of 3D modified copper mesh.[90] Reproduced with permission. Copyright 2023, Elsevier.

Cu current collector remained remarkably ordered and uniform, which resulted from a uniform Li^+ flux and an even voltage gradient for 3D Cu (Fig. 12g). Furthermore, Li *et al.* introduced a groundbreaking innovation with the development of a super-three-dimensional resorcinol formaldehyde copper mesh (referred to as a-RF@3D CM) using resorcinol formaldehyde. Resorcinol formaldehyde will first transform into amorphous carbon with function groups holding oxygen (Fig. 12h) and then be engineered onto copper mesh. This fabricated structure is filled with CuO_x nanoparticles, which use the attraction of oxygen ions from themselves to facilitate dendrite-less lithium coating. Consequently, an a-RF@3D CM whole cell coupled with the LFP cathode exhibits a retention capacity of 60.66% and an average coulombic efficiency of 99.5% over 100 cycles.[90] Besides, as displayed in Fig. 12i, the increased content of LiF and the decreased Li_2CO_3 signified that decomposition of organic electrolyte was suppressed. The emergence of three-dimensional current collectors has led to changes in the design and structure of the AFLMB, providing a direction to improve the flexibility of AFLMBs.

3.3 New materials for current collectors

Although copper remains the predominant material for anode current collectors, the investigation of other materials such as nickel, chromium and carbon nanofibers (CNFs) is gaining momentum. Moving to alternative materials provides a direct way to tune the lithium nucleation overpotential and lithium affinity of current collectors, with various Fermi levels influencing electron flow direction and electrolyte consumption control.

Kwon *et al.* reported multivacancy defective carbon paper (d-CP) current collectors which can improve the cycling stability of their corresponding AFLMBs.[91] Compared with cells assembled using pristine carbon paper (p-CP), cells employing d-CP CCs enjoyed a thinner and smoother SEI that is approximately one-third of the one formed in p-CP cells. Additionally, as shown in Fig. 13a, the SEI formed in the AFLMB with d-CP possesses a larger amount of LiF, indicating improved Li ion conductivity and flexibility compared with the control group. The obtained d-CP cell delivered a capacity retention of 90% at a current density of 2.0 mA cm^{-2} after 50 charge–discharge

Open Access Article. Published on 14 juin 2024. Downloaded on 2025-01-24 19:52:32.
This article is licensed under a Creative Commons Attribution-NonCommercial 3.0 Unported Licence.

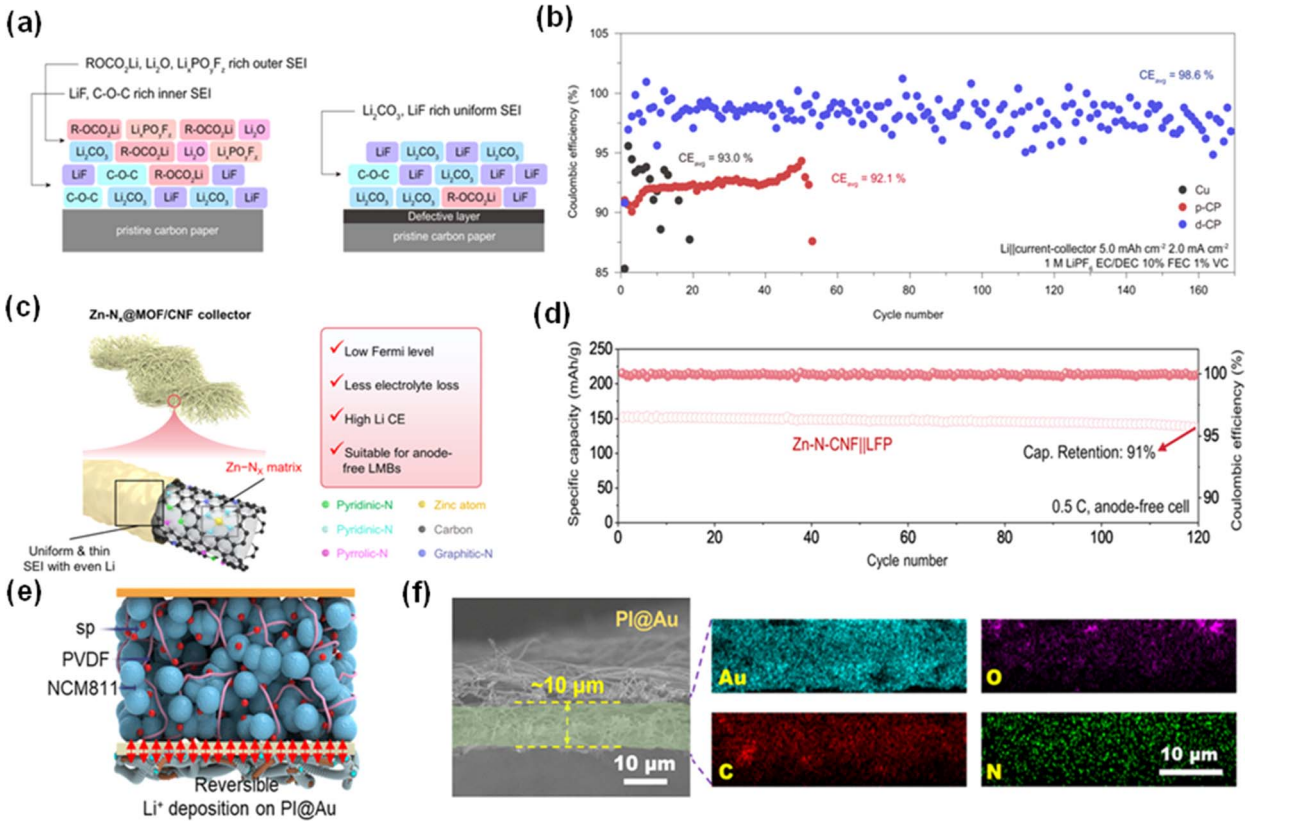

Fig. 13 New types of current collector and their performance. (a) The proposed SEI chemical composition on the p-CP CC and d-CP CC. (b) Li plating efficiency on bare Cu, p-CP and d-CP at 2 mA cm^{-2}.[91] Reproduced with permission. Copyright 2021, Springer Nature. (c) Advantages of the Zn–N-CNF CC over traditional CCs. (d) Cycling performance of a Zn–N-CNF||LFP full-cell over 120 cycles.[70] Reproduced with permission. Copyright 2024, Elsevier. (e) Reversible Li ion deposition on PI@Au. (f) Energy dispersive spectroscopy (EDS) images of PI@Au.[93] Reproduced with permission. Copyright 2023, Elsevier.

cycles. The ultralight 3D structures promise high gravimetric and volumetric densities and support the formation of a dendrite-free and dense lithium layer, significantly reducing the nucleation energy required for lithium deposition.[86,92] The AFLMBs employing these nanofibers have achieved impressive capacity retentions, indicating a substantial enhancement in battery life.

Zhang *et al.* designed a Zn–N-carbon nanofiber (Zn–N-CNF) for the anode CC of AFLMBs.[70] The obtained CC provides a lower Fermi level, which helps prevent the transfer of electrons to the electrolyte, consequently slowing electrolyte depletion. Fig. 13c demonstrates the advantages of Zn–N-CNF. The SEI formed in the Zn–N-CNF CC battery is much thinner than the one formed in the traditional system, indicating its inhibitory effect on electrolyte decomposition. Moreover, the lithiophilic properties of the material facilitate the formation of a more uniform and denser lithium deposition layer, which is vital for improving the performance of AFLMBs. Therefore, cells of the CC coupled with an LFP cathode exhibited a very satisfactory capacity retention of 91% after 120 cycles at 0.5C (Fig. 13d).

Wu *et al.* fabricated an ultralight (0.54 g cm^{-3}) 3D polyimide nanofiber with a thin Au coating (PI@Au), which represents another groundbreaking development.[93] Due to its low specific mass and thickness, exceedingly high gravimetric and volumetric densities can be achieved, 475 W h kg^{-1} and 1199 W h L^{-1} respectively, and its structure is shown in Fig. 13e. The EDS images in Fig. 13f indicate the uniform distribution of Au in the polyimide nanofiber. Unlike Cu foil CC, the 3D PI@Au CC will deposit lithium onto its nanofiber first and then form a dendrite-free and dense Li plane. Furthermore, during the Li plating process, a thin layer of gold will react with Li and form a gold–lithium alloy, thus largely reducing the nucleation power. Consequently, the AFLMB employing this PI@Au and a NCM811 cathode exhibited a capacity retention of 86% after 100 cycles, providing an areal capacity of 6.4 mA h cm^{-2}. The investigation of alternative anode current collector materials provides an excellent way to improve the performance and durability of AFLMBs. These advancements provide unique advantages such as improved cycling stability, reduced electrolyte consumption, and enhanced lithium deposition uniformity, enlarging the research area in the battery industry.

4. Key parameters to develop high-performance AFLMBs

In the pursuit of enhancing the cycling stability of anode-free lithium metal batteries, researchers face the dual challenge of

 This journal is © The Royal Society of Chemistry 2024

Open Access Article. Published on 14 juin 2024. Downloaded on 2025-01-24 19:52:32.
This article is licensed under a Creative Commons Attribution-NonCommercial 3.0 Unported Licence.

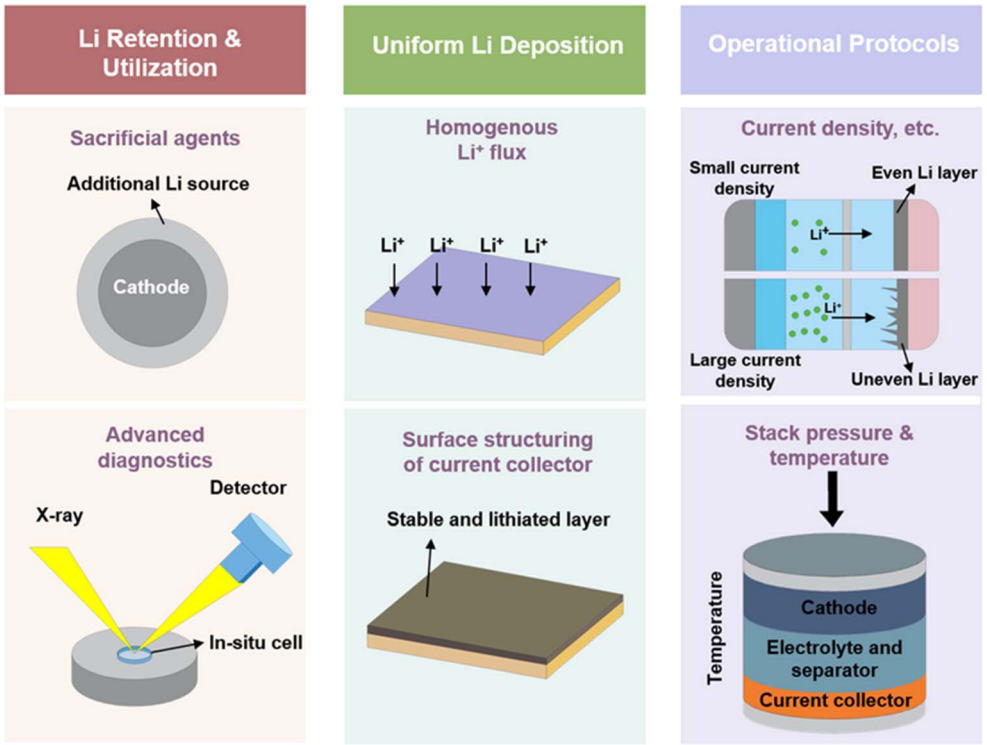

Fig. 14 Strategies for enhancing cycling stability in anode-free lithium metal batteries.

managing the limited supply of lithium and addressing the issues arising from inhomogeneous Li deposition. The configuration of AFLMBs offers multiple avenues for modification, each with the potential to significantly impact cell performance. Fig. 14 illustrates various research directions and acknowledges the ones associated with the efficacy of the cells. Research and development are prioritized, such as finding advanced diagnostic tools to better understand and improve battery performance and using cutting-edge technology for long battery life. Protocols, such as stack pressure and temperature during cycling are also considered, as they affect the electrode–electrolyte interface and ionic conductivity of AFLMBs deeply. Additionally, the detailed challenges of AFLMBs are summarized in Fig. 15.

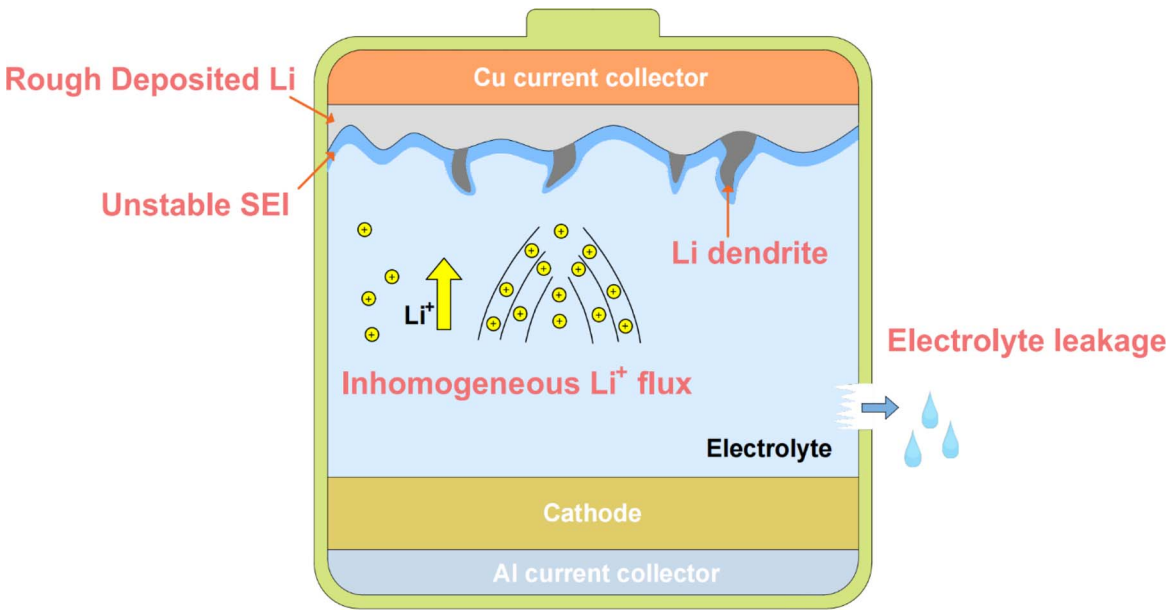

Fig. 15 Challenges of anode-free lithium metal batteries.

Open Access Article. Published on 14 juin 2024. Downloaded on 2025-01-24 19:52:32.
This article is licensed under a Creative Commons Attribution-NonCommercial 3.0 Unported Licence.

4.1 Enhancing lithium utilization and retention

One of the main goals of the development of AFLMBs is to maximize the utilization and retention of lithium. The pursuit of enhanced lithium utilization in AFLMBs is a multidimensional endeavor that integrates the development of electrolyte with the strategic use of sacrificial agents (Table 3).[94–96] This dual approach aims to mitigate lithium loss while improving cell efficiency, thereby improving the overall performance of AFLMBs. It is crucial that the introduction of sacrificial agents be meticulously managed to preclude deleterious reactions that could lead to gas formation, which imperils battery integrity.

In parallel, the stabilization of the solid-electrolyte interphase (SEI) is critical for the longevity of AFLMBs. By exploring electrolyte components and electrolyte additives, efforts are being made to fortify these interphases against strains from extensive cycling. These stable interphases are anticipated to sustain the integrity of battery operation, providing a reliable platform for efficient ion transport and extended battery life. Innovation in the current collector design is also critical to the advancement of AFLMBs. A range of strategies have been explored to improve the compatibility of current collectors with the lithium deposition process. From alloying copper with lithiophilic metals to applying conductive coatings and structuring surfaces at the micro or nanoscale, these efforts are geared towards promoting uniform lithium nucleation and circumventing dendrite formation. Moreover, the exploration of alternative materials such as zinc and titanium and three-dimensional current collectors is opening up new paths for performance benefits and potential cost reductions.[83] This transition is expected to bolster the overall stability of AFLMBs, marking a significant stride towards batteries that can reliably power the future.[94,97]

4.2 Pursuing homogeneity in lithium deposition

Inhomogeneous lithium deposition poses a significant challenge in optimizing anode-free lithium metal batteries, threatening battery structural integrity and cycling behavior. Addressing this issue requires focused modifications of current collectors, which are crucial for lithium plating. Strategies to enhance lithiophilicity, such as combining collectors with lithophilic materials or utilizing coatings and surface techniques, have been explored. However, ensuring modifications do not consume active lithium remains a challenge. Therefore, developing current collectors that sustain full lithiation throughout battery life is essential. Engineering inherently stable and fully lithiated current collectors from the outset is promising, aiming to avoid issues with fast lithium decay. Ultimately, these advancements can unlock the full potential of anode-free lithium metal batteries across various applications through innovative materials science and engineering.

4.3 Refining operational protocols for optimized performance

In the quest for optimized performance of anode-free lithium metal batteries, operational protocols play a decisive role,

Table 3 Overview of the future research directions for AFLMBs *via* enhancing lithium utilization and retention

Research focus	Strategies	Expected outcomes	Remarks
Enhancing lithium utilization	- Development of Li-rich cathodes - Use of sacrificial agents	- Reduced lithium loss - Improved cell efficiency	Excess lithium strategies should not compromise safety or battery performance
Stabilizing the SEI	- Advanced materials for the SEI - Electrolyte additives	- Stable interphases - Extended battery life	Robust SEI formation is critical for cycling stability and efficiency
Advanced diagnostics	- *In situ* and *ex situ* characterization tools - Real-time monitoring systems	- Better understanding of degradation mechanisms - Data-driven battery improvements	Diagnostic tools are essential for identifying failure modes and enabling predictive maintenance
Exploration of alternative materials	- Research on non-copper materials such as Zn and carbon-based materials - Evaluation of new lithiophilic compounds	- Alternative materials that possess higher affinity for Li - Novel properties such as reduced overpotential	Alternative materials should be both lithiophilic and low-cost
Addressing volume change and distribution	- Designing 3D current collectors - Developing materials that accommodate volume changes during cycling	- More uniform charge distribution - Increased surface area for lithium plating	3D current collectors may help alleviate stress within the battery, thus enhancing stability

This journal is © The Royal Society of Chemistry 2024

Open Access Article. Published on 14 juin 2024. Downloaded on 2025-01-24 19:52:32.
This article is licensed under a Creative Commons Attribution-NonCommercial 3.0 Unported Licence.

comparable in importance to the material components of the batteries themselves. The careful calibration of operational parameters such as stack pressure, cut-off voltage, and current density is essential in enhancing the battery's life span, improving coulombic efficiency, and ensuring overall performance. In addition, to ensure the ultra-thin structure of flexible anode-free lithium metal batteries, deep charge is often required.

Refining protocols involves a deep understanding of the electrochemical interplay within the battery system. For instance, stack pressure can significantly affect the intimate contact between the electrode and electrolyte, influencing the uniformity of lithium deposition and the integrity of the solid-electrolyte interphase (SEI).[59,60] Similarly, cut-off voltage settings are instrumental in defining the depth of discharge, which can prevent lithium depletion and mitigate the risk of dendrite formation, thereby prolonging battery life and maintaining safety standards. Indeed, experimental evidence from the work by Genovese *et al.* illustrates the delicate balance required in setting these parameters.[98]

Moreover, the ultra-thin structure of flexible AFLMBs necessitates a thorough analysis of how the depth of discharge (DoD) impacts battery performance. DoD is determined using a lower cutoff voltage, where reducing this cutoff voltage increases the battery capacity. Nevertheless, an increased DoD may adversely affect the cycling performance due to challenges in forming a stable lithium reservoir.[99] Typically, after the initial deep charge and discharge (1.25 V–4.5 V), anode-free batteries undergo cycling within a standard voltage range (3.5–4.5 V).[100] The lithium initially extracted from the cathode during the first charging cycle is deposited onto the current collector, creating a lithium reservoir. This reservoir compensates for lithium loss during cycling, consequently improving the battery's longevity. An intermittent high DoD protocol has been developed by researchers, where the battery predominantly cycles at a lower discharge depth of 50% and periodically experiences deeper discharges of 80%.[100] This strategy represents a balance between improving energy density and maintaining the lithium reservoir to extend the battery's cycle life. An alternative method involves a steady DoD, while implementing an asymmetric charging protocol that features a slower charge rate compared to the discharge rate.[101] This slower charging rate facilitates even lithium deposition, and the faster discharge rate will promote selective lithium extraction from the tip of the lithium reservoir, helping the removal of uneven Li deposits.[102]

The implication is clear: beyond the composition of the battery itself, the longevity and efficiency of AFLMBs can also be significantly influenced by operational protocols. This has been a new frontier in battery research, where the focus is not solely on material innovation but also on the refinement of cycling parameters. Such optimization requires rigorous testing and validation to establish protocols that not only maximize performance but also maintain it consistently over time. The future of AFLMBs thus hinges not only on the advancement of materials science but also on the strategic manipulation of operational parameters.

5. Challenges and strategies for implementing application of flexible AFLMBs

As mentioned earlier, the AFLMB possesses advantages such as high energy density, high power density, light weight, and high safety, making it a promising battery structure for the development of flexible devices. Addressing issues such as low coulombic efficiency and severe dendrite growth in AFLMBs, this review focuses on both the current research strategies and recent developments, primarily from the perspectives of the current collector and electrolyte. To further advance flexible AFLMBs for applications in wearable devices, artificial skin, and other flexible devices, considerations should also include the mechanical properties of the devices and safety concerns arising from bending. This section elaborates on potential directions and strategies for developing flexible AFLMBs (Fig. 16), focusing on electrolytes and current collectors, while also providing insights into the challenges encountered during the manufacturing process of AFLMBs.[103–106]

5.1 Gel polymers avoiding leakage under deformation

Liquid electrolytes are fundamental for uniform lithium metal deposition and exhibit high ionic conductivity, with lithium salts and organic solvents aiding in the formation of a solid electrolyte interface (SEI) layer. Nonetheless, their use in flexible AFLMBs presents significant safety risks. For instance, during frequent mechanical deformation of flexible devices, stress concentrates near bent areas, causing physical battery damage that may lead to electrolyte leakage and battery short circuits. Thus, gel and solid-state electrolytes prove more suitable for flexible devices. Ceramic solid-state electrolytes encounter challenges such as high brittleness, low ionic conductivity, and complex manufacturing processes. In contrast, gel electrolytes, comprising a polymer matrix and liquid electrolyte, offer both good ionic conductivity and mechanical flexibility, rendering them better suited for flexible devices.

The selection of polymer matrices and liquid electrolytes is crucial in designing gel electrolytes. Noteworthy electrolyte systems suitable for AFLMBs include Jeff Dahn's dual-salt electrolyte and Li *et al.*'s localized high-concentration electrolyte.[21,107] As for polymer matrices, options range from long-chain polymers such as PVDF-HFP to polymer monomers with vinyl functional groups such as PEGDA. Criteria for selecting these polymers encompass exhibiting good compatibility with the polymer matrix, maintaining stability with lithium, and preventing side reactions. Additionally, the polymer's spatial network should maximize electrolyte accommodation.

5.2 Current collector modification for high flexibility

In flexible AFLMBs, the current collector plays a crucial role not only in facilitating lithium deposition and stripping efficiency but also in maintaining the battery's flexibility and stability under repeated bending stress. In addition, lithium directly deposits onto the current collector in this system. Therefore, preventing

Open Access Article. Published on 14 juin 2024. Downloaded on 2025-01-24 19:52:32.
This article is licensed under a Creative Commons Attribution-NonCommercial 3.0 Unported Licence.

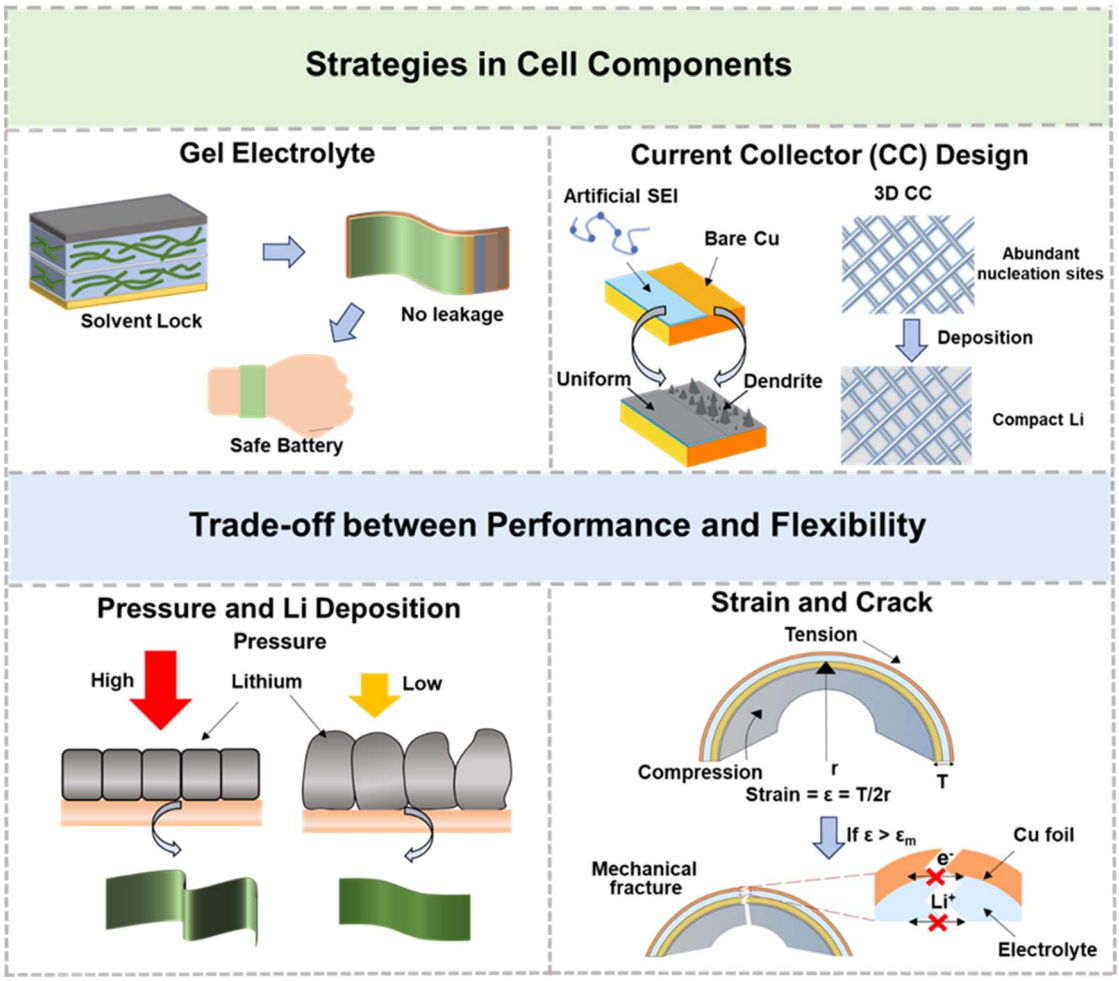

Fig. 16 Potential strategies and critical factors for implementing flexible anode-free lithium metal batteries.

lithium detachment from the current collector is essential in designing flexible AFLMBs. Generally, three-dimensional current collectors have a porous microstructure and abundant nucleation sites, enabling uniform lithium deposition/stripping while experiencing volume change. Moreover, 3D CCs are light weight and exhibit excellent mechanical flexibility. Therefore, the development of flexible three-dimensional current collectors is viewed as a promising strategy for realizing the application of flexible AFLMBs. Kandula *et al.* designed a nano-accordion framework using elastic $Ti_3C_2T_x$ and single-walled carbon nanotubes as the anode host.[108] Similarly, Gao *et al.* used carbon nanotubes and PVDF–HFP to create flexible and free-standing current collectors.[109] These innovative designs improve the cycling coulombic efficiency while increasing the flexibility of anode-free batteries. Such advancements are pivotal in the ongoing development of flexible anode-free batteries.

As previously mentioned, significant efforts have been dedicated to improving current collectors, aiming to design a stable SEI layer to achieve effective lithium plating and stripping. An ideal SEI in a flexible battery should possess good mechanical properties to withstand the expansion and contraction during lithium plating and stripping processes. Furthermore, the SEI should maintain adhesion to the current collector and its own integrity during battery cycling.[110] Furthermore, to accommodate the bending deformation of flexible devices, the SEI also needs to exhibit good flexibility. Therefore, polymer materials with excellent ion conductivity, processability, and high flexibility emerge as promising SEI materials for application in flexible AFLMBs. The selection of these ion-conducting polymer artificial SEI films is approached from four aspects: polymers with non-polar functional groups, polar functional groups, charged groups, and multiple ion-conducting functional groups.[111]

5.3 Trade-off between performance and flexibility

Research has shown that applying external pressure can effectively enhance the cycling lifespan of AFLMBs.[112] This is because pressure can efficiently constrain lithium growth and induce dendrite plastic deformation to maintain a flatter morphology and a lower surface area.[113] However, for flexible devices, applying significant external pressure is challenging as it compromises their flexibility.

During the repeated bending processes, the performance of flexible batteries is impacted by mechanical strain, which is

 This journal is © The Royal Society of Chemistry 2024

Open Access Article. Published on 14 juin 2024. Downloaded on 2025-01-24 19:52:32.
This article is licensed under a Creative Commons Attribution-NonCommercial 3.0 Unported Licence.

determined from both the radius of bending curvature and the battery's thickness.[114] The theoretical maximum strain (ε_m) in flexible batteries is proportional to the cell thickness (T), expressed using the formula:

$$\varepsilon_m = T/2r_b \quad (1)$$

The minimum radius of bending curvature is defined as r_b.[115,116] Generally, the maximum strain (ε_m) is a more reasonable parameter than r_b for evaluating the flexibility of battery components and batteries themselves. Larger strains experienced during bending can lead to irreversible plastic deformation, which impairs the integrity of electrodes, potentially causing cracking of the battery and thus increasing the internal resistance ε_m of the battery. Furthermore, mechanical stresses such as twisting can promote the growth of dendrites. Extensive dendrite formation not only diminishes battery capacity quickly but also increases the possibility of piercing the separator, leading to short circuits and raising safety issues.

Therefore, there is a need to balance mechanical pressure and flexibility. Researchers have developed a composite model to address issues related to mechanical strain in flexible batteries. In the model, a 3D current collector functions as a structural support and filler, while the electrode material acts as a matrix, effectively releasing stress applied to the matrix during bending processes.[117] Inspired by this, in flexible anode-free batteries, utilizing a 3D flexible current collector instead of a traditional copper current collector can not only provide active sites for uniform lithium deposition/stripping, improving battery lifespan and cycling stability but also reduce electrode thickness, enhancing the mechanical flexibility of flexible batteries. Another feasible approach is process improvement by selecting suitable casing/packaging. For instance, multi-layer packaging structures designed by Argonne National Laboratory and polymer package for thin batteries effectively protect the integrity of battery components.[118] These structures are expected to ensure flexibility in flexible AFLMB applications while effectively reducing battery capacity loss.

6. Conclusion

This review briefly summarizes the latest research progress of AFLMBs, focusing on the development of advanced current collectors and innovative electrolytes, aiming to explore the potential for developing flexible AFLMBs. The anode-free battery is characterized by light weight, low-cost, high-energy density, and high safety and has become the basis and premise for constructing ideal flexible devices. This review is based on the characteristics of flexible devices and selects the most suitable method for developing flexible anode-free batteries among various strategies towards enhancing the performance of anode-free batteries. It is concluded that the utilization of gel electrolytes and mechanically robust ion-conductive polymer artificial SEI layers effectively enhances the cycling life and flexibility of flexible AFLMBs. Simultaneously, innovative manufacturing processes ensure that flexible AFLMBs remain competitive in practical applications.

Conflicts of interest

All authors declare no competing financial or non-financial interests.

Acknowledgements

This work was supported by the Singapore Ministry of Education Tier 1 Grant (RG91/23) and A*STAR (Agency for Science, Technology and Research) under its LCERFI program (Award No. U2102d2002).

References

1 Z. Z. Tong, B. Bazri, S. F. Hu and R. S. Liu, *J. Mater. Chem. A*, 2021, **9**, 7396–7406.
2 A. Kushima, K. P. So, C. Su, P. Bai, N. Kuriyama, T. Maebashi, Y. Fujiwara, M. Z. Bazant and J. Li, *Nano Energy*, 2017, **32**, 271–279.
3 C. W. Ma, S. T. Weng, Y. X. Zhang, X. Y. Zhang, T. Liu, L. Liu, Z. G. Zhao, C. C. Liu, Z. K. Zhao, X. F. Wang, B. R. Wu, D. B. Mu and F. Wu, *Nano Lett.*, 2022, **22**, 9268–9274.
4 C. Heubner, S. Maletti, H. Auer, J. Hüttl, K. Voigt, O. Lohrberg, K. Nikolowski, M. Partsch and A. Michaelis, *Adv. Funct. Mater.*, 2021, **31**, 2106608.
5 A. P. Cohn, N. Muralidharan, R. Carter, K. Share and C. L. Pint, *Nano Lett.*, 2017, **17**, 1296–1301.
6 S. F. Huang, S. R. Lu, Y. Lv, N. R. Li, Z. W. Wu, G. Zhong, X. L. Ren, Y. F. Wang, B. Sun, Y. X. Huang, F. Y. Kang and Y. D. Cao, *Nano Res.*, 2023, **16**, 11473–11485.
7 X. C. Wang, Y. F. He, S. B. Tu, L. Fu, Z. H. Chen, S. Y. Liu, Z. Cai, L. Wang, X. M. He and Y. M. Sun, *Energy Storage Mater.*, 2022, **49**, 135–143.
8 W. Zhang, J. L. Zheng, Z. Ren, J. C. Wang, J. M. Luo, Y. Wang, X. Y. Tao and T. F. Liu, *Adv. Mater.*, 2024, **36**, 2310347.
9 L. Su, H. Charalambous, Z. Cui and A. Manthiram, *Energy Environ. Sci.*, 2022, **15**, 843–854.
10 A. Shao, X. Tang, M. Zhang, M. Bai and Y. Ma, *Adv. Energy Sustainability Res.*, 2022, **3**, 2100197.
11 B. Wu, C. Chen, L. H. J. Raijmakers, J. Liu, D. L. Danilov, R.-A. Eichel and P. H. L. Notten, *Energy Storage Mater.*, 2023, **57**, 508–539.
12 S. Nanda, A. Gupta and A. Manthiram, *Adv. Energy Mater.*, 2021, **11**, 2000804.
13 C.-H. Jo, K.-S. Sohn and S.-T. Myung, *Energy Storage Mater.*, 2023, **57**, 471–496.
14 S. Jurng, Z. L. Brown, J. Kim and B. L. Lucht, *Energy Environ. Sci.*, 2018, **11**, 2600–2608.
15 D. T. Boyle, W. Huang, H. Wang, Y. Li, H. Chen, Z. Yu, W. Zhang, Z. Bao and Y. Cui, *Nat. Energy*, 2021, **6**, 487–494.
16 D. Lin, Y. Liu, Y. Li, Y. Li, A. Pei, J. Xie, W. Huang and Y. Cui, *Nat. Chem.*, 2019, **11**, 382–389.
17 B. X. Zhou, I. Stosevski, A. Bonakdarpour and D. P. Wilkinson, *Adv. Funct. Mater.*, 2023, **34**, 2311212.

Open Access Article. Published on 14 juin 2024. Downloaded on 2025-01-24 19:52:32.
This article is licensed under a Creative Commons Attribution-NonCommercial 3.0 Unported Licence.

18 J. F. Qian, W. A. Henderson, W. Xu, P. Bhattacharya, M. Engelhard, O. Borodin and J. G. Zhang, *Nat. Commun.*, 2015, **6**, 6362.
19 D. C. Zhang, Y. X. Liu, Z. Y. Sun, Z. B. Liu, X. J. Xu, L. Xi, S. M. Ji, M. Zhu and J. Liu, *Angew. Chem., Int. Ed.*, 2023, **62**, e202310006.
20 Z. L. Brown and B. L. Lucht, *J. Electrochem. Soc.*, 2018, **166**, A5117–A5121.
21 R. Weber, M. Genovese, A. J. Louli, S. Hames, C. Martin, I. G. Hill and J. R. Dahn, *Nat. Energy*, 2019, **4**, 683–689.
22 N. H. Hawari, H. Q. Xie, A. Prayogi, A. Sumboja and N. Ding, *RSC Adv.*, 2023, **13**, 25673–25680.
23 X. Q. Min, C. X. Han, S. H. Zhang, J. Ma, N. F. Hu, J. D. Li, X. F. Du, B. Xie, H. J. Lin, C. Y. Kuo, C. T. Chen, Z. W. Hu, L. X. Qiao, Z. L. Cui, G. J. Xu and G. L. Cui, *Angew. Chem., Int. Ed.*, 2023, **62**, e202302664.
24 A. J. Louli, A. Eldesoky, R. Weber, M. Genovese, M. Coon, J. deGooyer, Z. Deng, R. T. White, J. Lee, T. Rodgers, R. Petibon, S. Hy, S. J. H. Cheng and J. R. Dahn, *Nat. Energy*, 2020, **5**, 693–702.
25 C. J. Niu, H. Lee, S. R. Chen, Q. Y. Li, J. Du, W. Xu, J. G. Zhang, M. S. Whittingham, J. Xiao and J. Liu, *Nat. Energy*, 2019, **4**, 551–559.
26 A. J. Louli, M. Genovese, R. Weber, S. G. Hames, E. R. Logan and J. R. Dahn, *J. Electrochem. Soc.*, 2019, **166**, A1291–A1299.
27 Z. Y. Lu, H. J. Yang, Q. H. Yang, P. He and H. S. Zhou, *Angew. Chem., Int. Ed.*, 2022, **61**, e202200410.
28 X. Ye, J. Wu, J. N. Liang, Y. P. Sun, X. Z. Ren, X. P. Ouyang, D. Z. Wu, Y. L. Li, L. Zhang, J. T. Hu, Q. L. Zhang and J. H. Liu, *ACS Appl. Mater. Interfaces*, 2022, **14**, 53788–53797.
29 T. T. Beyene, B. A. Jote, Z. T. Wondimkun, B. W. Olbassa, C. J. Huang, B. Thirumalraj, C. H. Wang, W. N. Su, H. J. Dai and B. J. Hwang, *ACS Appl. Mater. Interfaces*, 2019, **11**, 31962–31971.
30 T. T. Hagos, B. Thirumalraj, C. J. Huang, L. H. Abrha, T. M. Hagos, G. B. Berhe, H. K. Bezabh, J. Cherng, S. F. Chiu, W. N. Su and B. J. Hwang, *ACS Appl. Mater. Interfaces*, 2019, **11**, 9955–9963.
31 J. Qian, B. D. Adams, J. Zheng, W. Xu, W. A. Henderson, J. Wang, M. E. Bowden, S. Xu, J. Hu and J. G. Zhang, *Adv. Funct. Mater.*, 2016, **26**, 7094–7102.
32 Z. E. Feng, K. Higa, K. S. Han and V. Srinivasan, *J. Electrochem. Soc.*, 2017, **164**, A2434–A2440.
33 T. T. Beyene, H. K. Bezabh, M. A. Weret, T. M. Hagos, C.-J. Huang, C.-H. Wang, W.-N. Su, H. Dai and B.-J. Hwang, *J. Electrochem. Soc.*, 2019, **166**, A1501.
34 H.-H. Sun, A. Dolocan, J. A. Weeks, R. Rodriguez, A. Heller and C. B. Mullins, *J. Mater. Chem. A*, 2019, **7**, 17782–17789.
35 Y. Yamada, J. H. Wang, S. Ko, E. Watanabe and A. Yamada, *Nat. Energy*, 2019, **4**, 269–280.
36 M. L. Mao, X. Ji, Q. Y. Wang, Z. J. Lin, M. Y. Li, T. Liu, C. L. Wang, Y. S. Hu, H. Li, X. J. Huang, L. Q. Chen and L. M. Suo, *Nat. Commun.*, 2023, **14**, 1082.
37 J. Chen, Q. Li, T. P. Pollard, X. L. Fan, O. Borodin and C. S. Wang, *Mater. Today*, 2020, **39**, 118–126.
38 C. Niu, D. Liu, J. A. Lochala, C. S. Anderson, X. Cao, M. E. Gross, W. Xu, J.-G. Zhang, M. S. Whittingham, J. Xiao and J. Liu, *Nat. Energy*, 2021, **6**, 723–732.
39 B. L. Wu, C. G. Chen, D. L. Danilov, Z. Q. Chen, M. Jiang, R. A. Eichel and P. H. L. Notten, *Energy Environ. Mater.*, 2023, **7**, e12642.
40 A. Pei, G. Y. Zheng, F. F. Shi, Y. Z. Li and Y. Cui, *Nano Lett.*, 2017, **17**, 1132–1139.
41 Z. Yu, H. S. Wang, X. Kong, W. Huang, Y. C. Tsao, D. G. Mackanic, K. C. Wang, X. C. Wang, W. X. Huang, S. Choudhury, Y. Zheng, C. V. Amanchukwu, S. T. Hung, Y. T. Ma, E. G. Lomeli, J. Qin, Y. Cui and Z. N. Bao, *Nat. Energy*, 2020, **5**, 526–533.
42 Q. W. Yang, Z. Q. Zhang, X. G. Sun, Y. S. Hu, H. B. Xing and S. Dai, *Chem. Soc. Rev.*, 2018, **47**, 2020–2064.
43 H. Sun, G. Z. Zhu, Y. M. Zhu, M. C. Lin, H. Chen, Y. Y. Li, W. H. Hung, B. Zhou, X. Wang, Y. X. Bai, M. Gu, C. L. Huang, H. C. Tai, X. T. Xu, M. Angell, J. J. Shyue and H. J. Dai, *Adv. Mater.*, 2020, **32**, 2001741.
44 G. M. A. Girard, M. Hilder, N. Dupre, D. Guyomard, D. Nucciarone, K. Whitbread, S. Zavorine, M. Moser, M. Forsyth, D. R. MacFarlane and P. C. Howlett, *ACS Appl. Mater. Interfaces*, 2018, **10**, 6719–6729.
45 T. Pathirana, R. Kerr, M. Forsyth and P. C. Howlett, *Sustainable Energy Fuels*, 2021, **5**, 4141–4152.
46 P. Liang, H. Sun, C. L. Huang, G. Z. Zhu, H. C. Tai, J. C. Li, F. F. Wang, Y. Wang, C. J. Huang, S. K. Jiang, M. C. Lin, Y. Y. Li, B. J. Hwang, C. A. Wang and H. J. Dai, *Adv. Mater.*, 2022, **34**, 2207361.
47 D. H. S. Tan, Y. T. Chen, H. D. Yang, W. Bao, B. Sreenarayanan, J. M. Doux, W. K. Li, B. Y. Lu, S. Y. Ham, B. Sayahpour, J. Scharf, E. A. Wu, G. Deysher, H. E. Han, H. J. Hah, H. Jeong, J. B. Lee, Z. Chen and Y. S. Meng, *Science*, 2021, **373**, 1494.
48 N. A. Sahalie, Z. T. Wondimkun, W. N. Su, M. A. Weret, F. W. Fenta, G. B. Berhe, C. J. Huang, Y. C. Hsu and B. J. Hwang, *ACS Appl. Energy Mater.*, 2020, **3**, 7666–7679.
49 J. Lopez, A. Pei, J. Y. Oh, G. J. N. Wang, Y. Cui and Z. A. Bao, *J. Am. Chem. Soc.*, 2018, **140**, 11735–11744.
50 Y. H. Lin, L. T. Wu, Y. T. Zhan, J. C. Jiang, Y. L. Lee, J. S. Jan and H. S. Teng, *Energy Storage Mater.*, 2023, **61**, 102868.
51 W. Fan, N. W. Li, X. L. Zhang, S. Y. Zhao, R. Cao, Y. Y. Yin, Y. Xing, J. N. Wang, Y. G. Guo and C. J. Li, *Adv. Sci.*, 2018, **5**, 1800559.
52 J. Castillo, A. Santiago, X. Judez, I. Garbayo, J. A. C. Clemente, M. C. Morant-Miñana, A. Villaverde, J. A. González-Marcos, H. Zhang, M. Armand and C. M. Li, *Chem. Mater.*, 2021, **33**, 8812–8821.
53 G. H. Chen, F. Zhang, Z. M. Zhou, J. R. Li and Y. B. Tang, *Adv. Energy Mater.*, 2018, **8**, 1801219.
54 R. Xu, X. B. Cheng, C. Yan, X. Q. Zhang, Y. Xiao, C. Z. Zhao, J. Q. Huang and Q. Zhang, *Matter*, 2019, **1**, 317–344.
55 Y. Nikodimos, W. N. Su, K. N. Shitaw, S. K. Jiang, L. H. Abrha, M. A. Weret, S. K. Merso, T. M. Hagos, C. J. Huang, K. Lakshmanan, W. H. Huang, C. Y. Chang, J. M. Lin, S. H. Wu, C. C. Yang and B. J. Hwang, *Energy Storage Mater.*, 2023, **61**, 102861.

 This journal is © The Royal Society of Chemistry 2024

Open Access Article. Published on 14 juin 2024. Downloaded on 2025-01-24 19:52:32.
This article is licensed under a Creative Commons Attribution-NonCommercial 3.0 Unported Licence.

56 X. Q. Zhang, C. Z. Zhao, J. Q. Huang and Q. Zhang, *Engineering*, 2018, **4**, 831–847.
57 Y.-H. Lin, R. Subramani, Y.-T. Huang, Y.-L. Lee, J.-S. Jan, C.-C. Chiu, S.-S. Hou and H. Teng, *J. Mater. Chem. A*, 2021, **9**, 5675–5684.
58 Y.-H. Lin, C.-Y. Shih, R. Subramani, Y.-L. Lee, J.-S. Jan, C.-C. Chiu and H. Teng, *J. Mater. Chem. A*, 2022, **10**, 4895–4905.
59 B. D. Adams, E. V. Carino, J. G. Connell, K. S. Han, R. G. Cao, J. Z. Chen, J. M. Zheng, Q. Y. Li, K. T. Mueller, W. A. Henderson and J. G. Zhang, *Nano Energy*, 2017, **40**, 607–617.
60 S. Eijima, H. Sonoki, M. Matsumoto, S. Taminato, D. Mori and N. Imanishi, *J. Electrochem. Soc.*, 2019, **166**, A5421–A5429.
61 N. A. Sahalie, A. A. Assegie, W.-N. Su, Z. T. Wondimkun, B. A. Jote, B. Thirumalraj, C.-J. Huang, Y.-W. Yang and B.-J. Hwang, *J. Power Sources*, 2019, **437**, 226912.
62 Y. Liu, X. Meng, Z. Wang and J. Qiu, *Nat. Commun.*, 2022, **13**, 4415.
63 Y.-G. Lee, S. Fujiki, C. Jung, N. Suzuki, N. Yashiro, R. Omoda, D.-S. Ko, T. Shiratsuchi, T. Sugimoto, S. Ryu, J. H. Ku, T. Watanabe, Y. Park, Y. Aihara, D. Im and I. T. Han, *Nat. Energy*, 2020, **5**, 299–308.
64 J. Wen, T. Wang, C. Wang, Y. Dai, Z. Song, X. Liu, Q. Yu, X. Zheng, J. Ma, W. Luo and Y. Huang, *Adv. Mater.*, 2024, **36**, 2307732.
65 M. J. Wang, E. Carmona, A. Gupta, P. Albertus and J. Sakamoto, *Nat. Commun.*, 2020, **11**, 5201.
66 W. Huang, K. Yoshino, S. Hori, K. Suzuki, M. Yonemura, M. Hirayama and R. Kanno, *J. Solid State Chem.*, 2019, **270**, 487–492.
67 Y. Kato, S. Hori, T. Saito, K. Suzuki, M. Hirayama, A. Mitsui, M. Yonemura, H. Iba and R. Kanno, *Nat. Energy*, 2016, **1**, 16030.
68 W.-Z. Huang, C.-Z. Zhao, P. Wu, H. Yuan, W.-E. Feng, Z.-Y. Liu, Y. Lu, S. Sun, Z.-H. Fu, J.-K. Hu, S.-J. Yang, J.-Q. Huang and Q. Zhang, *Adv. Energy Mater.*, 2022, **12**, 2201044.
69 M. N. Lei, Z. Y. You, L. B. Ren, X. R. Liu and J. G. Wang, *J. Power Sources*, 2020, **463**, 228191.
70 X.-L. Zhang, L. Ma, Y.-P. Cai, J. Fransaer and Q. Zheng, *Matter*, 2023, **7**, 583–602.
71 S. Liu, X. Xia, Y. Zhong, S. Deng, Z. Yao, L. Zhang, X.-B. Cheng, X. Wang, Q. Zhang and J. Tu, *Adv. Energy Mater.*, 2018, **8**, 1702322.
72 Y. K. Huang, H. Y. Chen and L. Nyholm, *Small*, 2023, **19**, 2306829.
73 K. Yan, Z. D. Lu, H. W. Lee, F. Xiong, P. C. Hsu, Y. Z. Li, J. Zhao, S. Chu and Y. Cui, *Nat. Energy*, 2016, **1**, 16010.
74 Z. T. Wondimkun, W. A. Tegegne, J. Shi-Kai, C.-J. Huang, N. A. Sahalie, M. A. Weret, J.-Y. Hsu, P.-L. Hsieh, Y.-S. Huang, S.-H. Wu, W.-N. Su and B. J. Hwang, *Energy Storage Mater.*, 2021, **35**, 334–344.
75 L. D. Lin, L. M. Suo, Y. S. Hu, H. Li, X. J. Huang and L. Q. Chen, *Adv. Energy Mater.*, 2021, **11**, 2003709.
76 Y. Li, M. Bu, C. Mu and C. Yang, *Mater. Lett.*, 2024, **355**, 135449.
77 S. S. Zhang, X. Fan and C. Wang, *Electrochim. Acta*, 2017, **258**, 1201–1207.
78 Z. B. Zhang, H. Luo, Z. Y. Liu, S. H. Wang, X. F. Zhou and Z. P. Liu, *J. Mater. Chem. A*, 2022, **10**, 9670–9679.
79 X. Gu, J. Dong and C. Lai, *Eng. Rep.*, 2021, **3**, e12339.
80 H. Zhang, X. Liao, Y. Guan, Y. Xiang, M. Li, W. Zhang, X. Zhu, H. Ming, L. Lu, J. Qiu, Y. Huang, G. Cao, Y. Yang, L. Mai, Y. Zhao and H. Zhang, *Nat. Commun.*, 2018, **9**, 3729.
81 M.-k. Song, J.-H. Yim, S.-H. Baek and J.-w. Lee, *Appl. Surf. Sci.*, 2022, **588**, 152935.
82 H.-y. Xia, Y.-k. Wang and Z.-w. Fu, *Appl. Surf. Sci.*, 2023, **617**, 156529.
83 Y. Zhu, S. Wu, L. Zhang, B. Zhang and B. Liao, *ACS Appl. Mater. Interfaces*, 2023, **15**, 43145–43158.
84 O. Tamwattana, H. Park, J. Kim, I. Hwang, G. Yoon, T. H. Hwang, Y. S. Kang, J. Park, N. Meethong and K. Kang, *ACS Energy Lett.*, 2021, **6**, 4416–4425.
85 A. A. Assegie, J. H. Cheng, L. M. Kuo, W. N. Su and B. J. Hwang, *Nanoscale*, 2018, **10**, 6125–6138.
86 T. Zhao, S. W. Li, Y. Z. Wang, H. L. Wang, M. Zhang, X. Y. Tang, F. Liu, D. Du, H. Q. Zheng and Y. Ma, *J. Mater. Chem. A*, 2021, **9**, 21281–21290.
87 J. Kim, G. R. Lee, R. B. K. Chung, P. J. Kim and J. Choi, *Energy Storage Mater.*, 2023, **61**, 102899.
88 E. Adhitama, A. D. Refino, T. Brake, J. Pleie, C. Schmidt, F. Demelash, K. Neuhaus, S. Bornemann, S. Wiemers-Meyer, E. Peiner, M. Winter, H. S. Wasisto and T. Placke, *J. Mater. Chem. A*, 2023, **11**, 7724–7734.
89 E. Kim, W. Choi, S. Ryu, Y. Yun, S. Jo and J. Yoo, *J. Alloys Compd.*, 2023, **966**, 171393.
90 N. Li, T. Jia, Y. Liu, Y. Ouyang, Y. Lv, G. Zhong, Y. Wang, B. Sun, S. Lu, S. Huang, F. Kang and Y. Cao, *Mater. Today Energy*, 2023, **36**, 101341.
91 H. Kwon, J. H. Lee, Y. Roh, J. Baek, D. J. Shin, J. K. Yoon, H. J. Ha, J. Y. Kim and H. T. Kim, *Nat. Commun.*, 2021, **12**, 5537.
92 P. Qing, Z. B. Wu, Y. J. Chen, F. C. Tang, H. Yang and L. B. Chen, *J. Energy Chem.*, 2022, **72**, 151–157.
93 W. Wu, D. Ning, J. H. Zhang, G. D. Liu, L. X. Zeng, H. D. Yao, M. Wang, L. B. Deng and L. Yao, *Energy Storage Mater.*, 2023, **63**, 102974.
94 L. W. Dong, S. H. Zhang, D. H. Song, Y. P. Liu and C. H. Yang, *Chem. Eng. J.*, 2023, **454**, 140029.
95 Y. Qiao, H. J. Yang, Z. Chang, H. Deng, X. Li and H. S. Zhou, *Nat. Energy*, 2021, **6**, 653–662.
96 B. A. Jote, K. N. Shitaw, M. A. Weret, S. C. Yang, C. J. Huang, C. H. Wang, Y. T. Weng, S. H. Wu, W. N. Su and B. J. Hwang, *J. Power Sources*, 2022, **532**, 231303.
97 A. T. S. Freiberg, J. Sicklinger, S. Solchenbach and H. A. Gasteiger, *Electrochim. Acta*, 2020, **346**, 136271.
98 M. Genovese, A. J. Louli, R. Weber, S. Hames and J. R. Dahn, *J. Electrochem. Soc.*, 2018, **165**, A3321.
99 P. Dan, E. Mengeritsky, D. Aurbach, I. Weissman and E. Zinigrad, *J. Power Sources*, 1997, **68**, 443–447.

Open Access Article. Published on 14 juin 2024. Downloaded on 2025-01-24 19:52:32.
This article is licensed under a Creative Commons Attribution-NonCommercial 3.0 Unported Licence.

100 A. Louli, M. Coon, M. Genovese, J. Degooyer, A. Eldesoky and J. Dahn, *J. Electrochem. Soc.*, 2021, **168**, 020515.
101 A. Louli, A. Eldesoky, J. deGooyer, M. Coon, C. Aiken, Z. Simunovic, M. Metzger and J. Dahn, *J. Electrochem. Soc.*, 2022, **169**, 040517.
102 A. Mistry, C. Fear, R. Carter, C. T. Love and P. P. Mukherjee, *ACS Energy Lett.*, 2018, **4**, 156–162.
103 T. Zhou, Y. Zhao, J. W. Choi and A. Coskun, *Angew. Chem., Int. Ed.*, 2021, **60**, 22791–22796.
104 K. Heo, J. Im, S. Kim, C.-K. Lee, D. R. Chang, J. Kim, J.-W. Lee and J. Lim, *J. Ind. Eng. Chem.*, 2020, **81**, 278–286.
105 H. Ota, S. Emaminejad, Y. Gao, A. Zhao, E. Wu, S. Challa, K. Chen, H. M. Fahad, A. K. Jha, D. Kiriya, W. Gao, H. Shiraki, K. Morioka, A. R. Ferguson, K. E. Healy, R. W. Davis and A. Javey, *Adv. Mater. Technol.*, 2016, **1**, 1600013.
106 H.-S. Lim, D. T. Nguyen, J. A. Lochala, X. Cao and J.-G. Zhang, *ACS Energy Lett.*, 2024, **9**, 126–135.
107 C. M. Efaw, Q. Wu, N. Gao, Y. Zhang, H. Zhu, K. Gering, M. F. Hurley, H. Xiong, E. Hu, X. Cao, W. Xu, J.-G. Zhang, E. J. Dufek, J. Xiao, X.-Q. Yang, J. Liu, Y. Qi and B. Li, *Nat. Mater.*, 2023, **22**, 1531–1539.
108 S. Kandula, E. Kim, C. W. Ahn, J. Lee, B. Yeom, S. W. Lee, J. Cho, H.-K. Lim, Y. Lee and J. G. Son, *Energy Storage Mater.*, 2023, **63**, 103024.
109 C. Gao, J. Wang, Y. Huang, Z. Li, J. Zhang, H. Kuang, S. Chen, Z. Nie, S. Huang, W. Li, Y. Li, S. Jin, Y. Pan, T. Long, J. Luo, H. Zhou and X. Wang, *Nanoscale*, 2021, **13**, 10100–10107.
110 W. Liu, P. Liu and D. Mitlin, *Adv. Energy Mater.*, 2020, **10**, 2002297.
111 S. Gao, F. Sun, N. Liu, H. Yang and P.-F. Cao, *Mater. Today*, 2020, **40**, 140–159.
112 D. P. Wilkinson, H. Blom, K. Brandt and D. Wainwright, *J. Power Sources*, 1991, **36**, 517–527.
113 C. Xu, Z. Ahmad, A. Aryanfar, V. Viswanathan and J. R. Greer, *Proc. Natl. Acad. Sci. U. S. A.*, 2017, **114**, 57–61.
114 J. Chang, Q. Huang, Y. Gao and Z. Zheng, *Adv. Mater.*, 2021, **33**, 2004419.
115 J. Peng and G. J. Snyder, *Science*, 2019, **366**, 690–691.
116 J. Chang, Q. Huang and Z. Zheng, *Joule*, 2020, **4**, 1346–1349.
117 J. Jin, J. H. Ko, S. Yang and B. S. Bae, *Adv. Mater.*, 2010, **22**, 4510–4515.
118 E. Foreman, W. Zakri, M. Hossein Sanatimoghaddam, A. Modjtahedi, S. Pathak, A. G. Kashkooli, N. G. Garafolo and S. Farhad, *Adv. Sustainable Syst.*, 2017, **1**, 1700061.

This journal is © The Royal Society of Chemistry 2024